DESIGN AND SYNTHESIS OF A VHF SURFACE ACOUSTIC WAVE OSCILLATOR

DESIGN AND SYNTHESIS OF A VHF SURFACE ACOUSTIC WAVE OSCILLATOR

by

Dieter G. Seiler, B. Eng.

A Thesis

Submitted to the Faculty of Graduate Studies

In Partial Fulfillment of the Requirements

for the Degree

Master of Engineering

McMaster University

December 1975

MASTER OF ENGINEERING (1975) McMASTER UNIVERSITY
(Electrical Engineering) Hamilton, Ontario

TITLE: Design and Synthesis of a VHF Surface Acoustic Wave Oscillator

AUTHOR: Dieter G. Seiler, B. Eng. (McMaster University)

SUPERVISOR: Professor C.K. Campbell

NUMBER OF PAGES: ix; 97

Scope and Contents:

A 124 MHz surface acoustic wave delay line oscillator was fabricated and tested for its stability, output power and spectral response. The theory and design of the oscillator is covered, along with possible improvements which may lead to more efficient designs.

ABSTRACT

This thesis covers the design and fabrication of a Surface Acoustic Wave (SAW) oscillator. The oscillator was designed to operate at 124 MHz in the fundamental mode and was constructed on an ST-X quartz substrate. The type of SAW oscillator incorporated was of the delay line type where a SAW delay line is inserted in the feedback loop of an amplifier with excess gain. The delay line exhibited a bandpass characteristic with an insertion loss of 32 dB. The oscillator has a short-term stability of 2.0 parts in 10^7 over 1 second and a medium-term stability of less than 8 ppm over 12 hours. The oscillator had an effective loaded Q of 628 and power output was -10 dBm into 50 Ω with the second harmonic down 22 dB, and the third down 33 dB. The theory of operation of the SAW delay line oscillator is covered along with fabrication procedures and experimental results.

ACKNOWLEDGEMENTS

The author would like to give special thanks to Dr. C.K. Campbell, who as the thesis supervisor provided valuable discussion time and a willingness to provide all that was necessary for the work done in this thesis.

The author would also like to thank Dr. V.M. Ristic from the University of Toronto for the two Microwave Acoustics courses which the author attended and for his inspiration and interest which he gave the author in the field of surface acoustic waves.

Next, the author would like to thank Dr. S.S. Haykin for the use of the Communications Research Laboratory facilities. Special thanks go to Mr. M. Suthers who provided much helpful discussion and interest in the work done for this thesis. The author also thanks Mr. P. Edmonson, Mr. S. Ogletree, and Mr. M. El-Diwany for their technical assistance and helpful discussions.

Finally, the author thanks B. Paré for her expert typing of this thesis in record time.

TABLE OF CONTENTS

TABLE OF CONTENTS Continued.

LIST OF FIGURES

CHAPTER I

INTRODUCTION

1.1 Scope of this Thesis

Surface Acoustic Wave (SAW) devices are becoming more popular as their relative advantages are being put to greater use. The small wavelengths involved allow signal processing functions to take place on substrates many times smaller and more practical than their electromagnetic or digital counterparts. One such device is the SAW oscillator which offers advantages in size and performance and shows great promise in future development. This thesis will cover the analysis, design and fabrication of a SAW oscillator. The detailed theory and physics of acoustic waves is beyond the scope of this thesis and is covered in [1]. Similarly, there are many aspects of SAW devices and theory which will not be dealt with in this thesis but are covered elsewhere. [2],[3]. Only the pertinent parameters concerning SAW oscillators will be covered, with emphasis on the engineering aspects of SAW's.

1.2 Surface Acoustic Waves

A surface acoustic wave is an elastic or mechanical wave which travels along a specified path on the surface of a substrate. The velocity of propagation of these acoustic waves ranges from 3000 m/sec. to 4000 m/sec. for the most common substrates and is primarily a function of the type of substrate used. This fact therefore allows a reduction in wavelength on the order of 10^5 times for acoustic waves relative to

electromagnetic waves. Since most of the wave energy is confined to a depth of one wavelength [4] below the surface and the wavelengths are quite small, ($\sim$ 30 μm for 100 MHz signals) it is valid to say that the bulk of the energy is contained in the surface of the material.

In order to create these surface acoustic waves a generator of some kind must be used. This generator is usually in the form of a transducer which converts electrical signals into mechanical displacements. For efficient conversion of energy the substrate must be piezoelectric, in which case an electric field propagates along with the acoustic wave on the surface. This electric field extends out into the free space above the surface and can therefore react with any electrodes placed on the surface. The Interdigital Transducer (IDT) makes use of this fact to generate, tap and detect acoustic waves on piezoelectric substrates. The IDT is the most commonly used transducer for SAW devices and is shown in Figure 1.1.

The IDT basically consists of parallel strips deposited on the surface with width d and a centre-to-centre spacing L. These conducting strips are called "fingers" and are electrically connected in the manner shown in Figure 1.1. When excited with an r.f. signal an electric field is set-up in the substrate surface as represented for one instant in time in Figure 1.2. Since the substrate is piezoelectric, this electric field causes deformations in the material due to stresses and strains acting on the substrate surface. With an alternating electric field, these deformations become periodic waves travelling away from the fingers in both directions, the period being defined by:

$$\lambda_o = 2L = \frac{v_a}{f_o} \qquad (1.1)$$

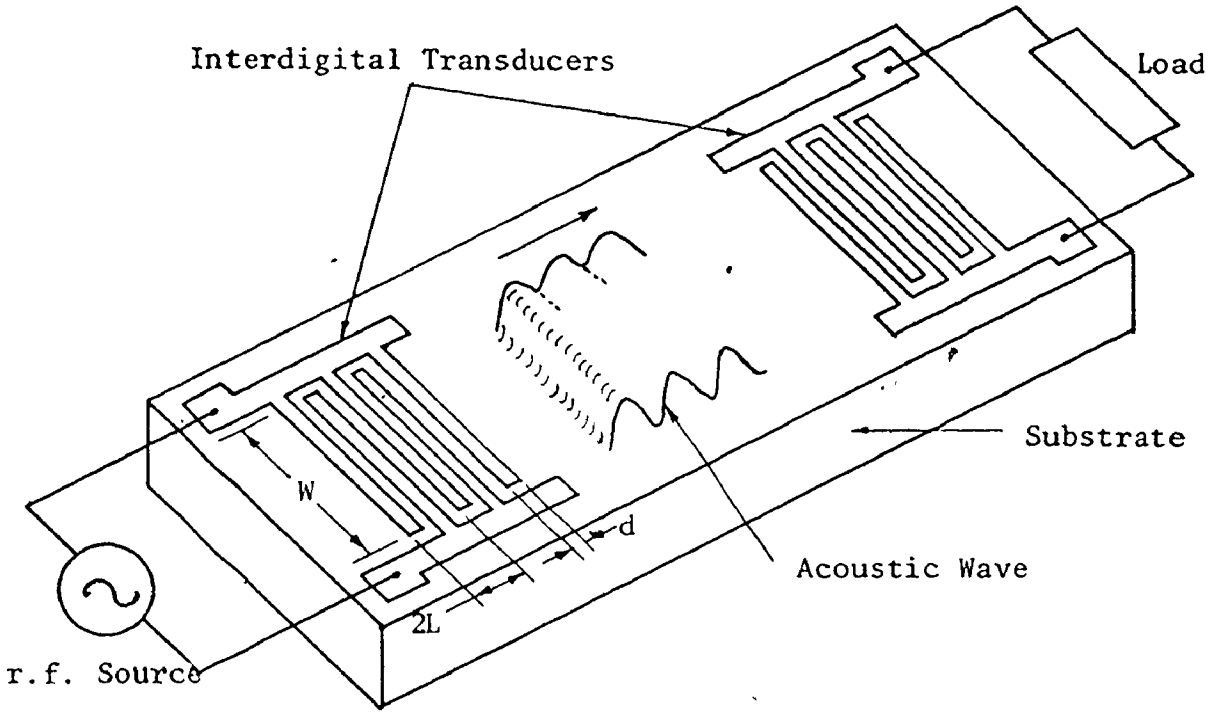

Figure 1.1 Basic Transducer Configuration for Generation and Detection of SAW's

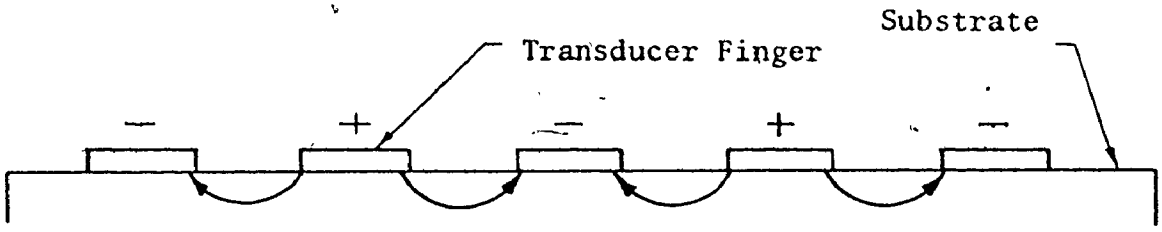

Figure 1.2 Electric Field Pattern of SAW Transducer

where λ_o = acoustic wavelength

L = centre-to-centre spacing of fingers

v_a = velocity of acoustic surface wave

f_o = acoustic synchronous frequency

The inverse also holds true for an acoustic wave travelling under the fingers of an output transducer. Therefore SAW propagation can be considered a transmitting and receiving system with all the signal processing taking place in the acoustic medium. Equation (1.1) shows that the design frequency is implemented by choice of the distance L, and if the fundamental mode is to be excited then the finger widths will become L/2. (i.e. unity width-to-gap ratio) The frequency f_o is termed synchronous since the transducers are centred on this frequency and therefore the induced voltages at the output fingers will add in phase and yield a maximum output at f_o.

If an impulse is applied to the input transducer, the resulting acoustic wave approximates the shape of a sine wave due to the stress-strain properties of the substrate between the fingers. As this acoustic sine wave passes beneath the output transducer (of similar design to the input transducer) a voltage is induced which in time is one cycle of a sine wave with frequency $f_o = \frac{v_a}{2L}$. The amplitude of the response is proportional to the finger overlap W of the transducers. Hence the output of the system is the impulse response of the SAW circuit. This is a basic point in SAW design since the resulting frequency response is calculated by taking the Fourier transform of the impulse response. In the general design case the desired frequency response is specified from which the corresponding impulse response is obtained by means of the

Inverse Fourier Transform (IFT). The remaining task is to design the transducers in such a way as to approximate the time response as accurately as possible by adjusting the transducer length, aperture W, spacing L, width d and finally the substrate material.

Many variations in transducer design exist, including apodized (variable aperture) transducers, but the simplest design consists of N finger pairs with a constant finger spacing L_o, aperture W_o and total length equivalent in time to $t = t_o$ with the phase centre of the array at $t = t_o/2$. The impulse response of this transudcer is $W_o \cos \omega_o t$ where $\omega_o = \pi v_a/L_o$. Therefore the frequency response of this simple transducer is given by [5]:

$$F_1(\omega) = \int_{-t_o/2}^{t_o/2} W_o \cos \omega_o t \, e^{-j\omega t} \, dt$$

$$\approx K t_o \frac{\sin(\omega_o - \omega)t_o/2}{(\omega_o - \omega)t_o/2} \qquad (1.2)$$

where K = scaling constant dependent on aperture W_o, substrate material, etc.

The frequency response is seen to be of the sin x/x form and therefore the simple transducer exhibits a bandpass characteristic in the frequency domain. As the transducer length is increased (i.e. more fingers are added) the resonant response increases and the bandwidth becomes narrower. The practical frequency range for SAW devices is from approximately 10 MHz to 2 GHz, limited on the low end by available substrate size and on the high end by fabrication tolerances and propagation losses. By apodizing the finger structure of a transducer one

can realize band-pass filters and a variety of other devices. [2]. The simple transducer system is used primarily as a delay line because of the slow surface wave velocities. However, many variations on the simple delay line exist including tapped delay lines and resonator structures. These variations have been exploited in the area of SAW oscillators which is making the SAW oscillator a comparable performer to bulk wave oscillators.

1.3 SAW Oscillators

Conventional bulk wave crystal oscillators have fundamental frequencies up to 30 MHz and become more fragile as the frequency is increased. Harmonic operation and multiplication must be used to obtain higher microwave frequencies. SAW oscillators have fundamental operation up to 1 GHz using conventional photolithographic techniques and with electron beam techniques this can be extended up to a few gigahertz. This eliminates any possible collective noise from transistor multiplier chains and also makes SAW oscillators space-qualified. Since the substrate itself does not oscillate it can be firmly mounted to yield a rugged device with a fairly high power capability. SAW devices are manufactured using planar techniques which make them compatible with integrated circuits and allow an overall reduction in physical size. SAW oscillators also offer a greater depth of modulation capability of greater than 2% compared to 0.1% for bulk quartz oscillators. A summary [6] of the SAW oscillator properties compared to bulk wave and LC oscillators is given in Figure 1.3.

The AT-cut quartz bulk wave oscillator is presently still superior to the SAW oscillator in the area of stability and long term

Oscillator	Approximate Frequency Range	Effective Loaded Q	Max. Freq. Deviation ppm	Temp. Coeff. in ppm/°C (-30°C to +70°C)
Conventional Quartz Crystal	$<10^8$ Hz	$5000\text{-}2\times10^6$	≈500	<1ppm/°C
LC (including cavity osc.)	$10^3\text{-}10^{11}$ Hz	Typically $10\text{-}10^4$	as large as required	Typically 10ppm/°C
SAW	$10^7\text{-}2\times10^9$ Hz	$200\text{-}10^4$ by choice of ℓ	$10^2\text{-}10^4$ by choice of ℓ	average value ≈1ppm/°C

Figure 1.3 Comparison of Properties of Various Oscillators

PARAMETER	SPECIFICATION
Frequency	500 MHz
Short-Term Stability (over 1/4 second)	1 in 10^{10}
Long-Term Stability (over 3 years)	1 in 10^6
Temperature Stability (over -10°C to +50°C)	1 in 10^6
Output Power	5 mW
Overall Efficiency	>1 percent

Figure 1.4 Space-Qualified Local Oscillator Drive Specifications

aging. Typical local oscillator drive specifications [7] are shown in Figure 1.4 and it is expected that SAW oscillators will meet these demands in the near future.

The most common type of SAW oscillator is the delay-line type which was developed by the Royal Radar Establishment. [8]. Figure 1.5 shows the system schematic for this type of oscillator. Basically the frequency selectivity and delay time of a SAW delay line are used in the feedback loop of an amplifier which provides excess gain to overcome the losses in the delay line. Two basic types of transducer geometry are used for the delay line, and are shown in Figure 1.6. The shorter geometry is ideal where substrate area is limited while the longer staggered delay line offers increased stability due to the increased Q of the filter and the long acoustic propagation times involved. Alternatively, two smaller transducers staggered by $\lambda_s/4$ can be positioned on the opposite side of the input transducer to obtain phase quadrature outputs if desired.

Harmonic operation of a delay line SAW oscillator is also possible and has recently been shown to be quite effective. [9]. Original work in this area was prompted by H. Engan in [10]. A plot of the amplitudes of the various space harmonics as a function of a is shown in Figure 1.7 where

$a = d/L$

d = finger width

L = centre-to-centre finger spacing

The author in [9] has produced similar plots for 3 and 4 finger-per-wavelength transducers and has shown that the advantages of these transducer

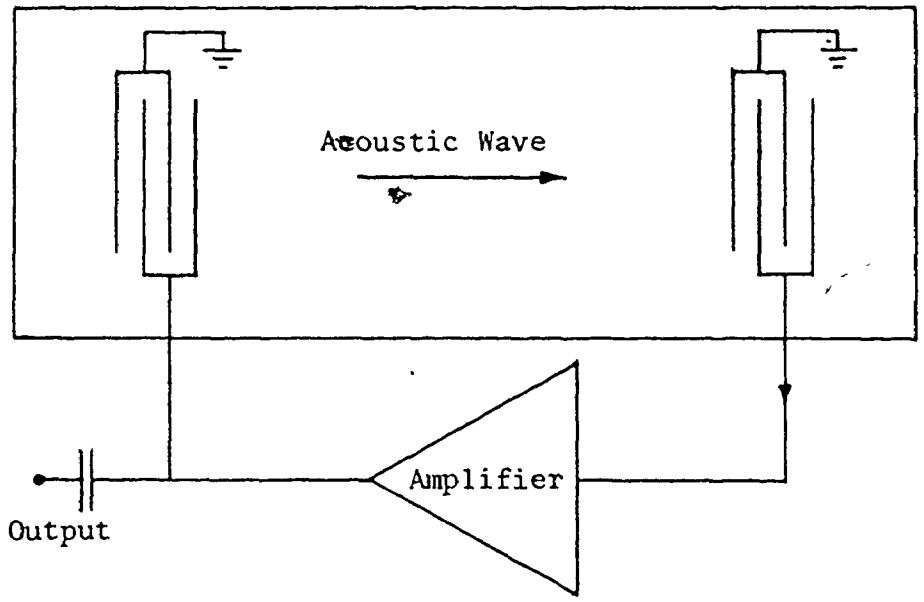

Figure 1.5 Schematic of SAW Oscillator with Delay Line

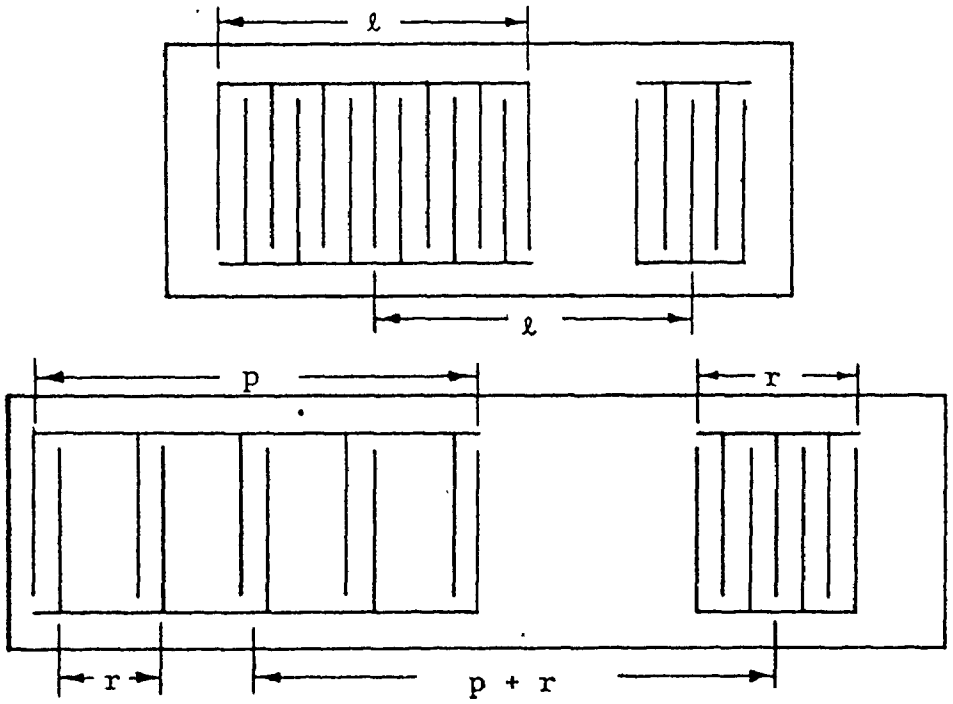

Figure 1.6 Two Basic Types of Delay Lines for SAW Oscillators

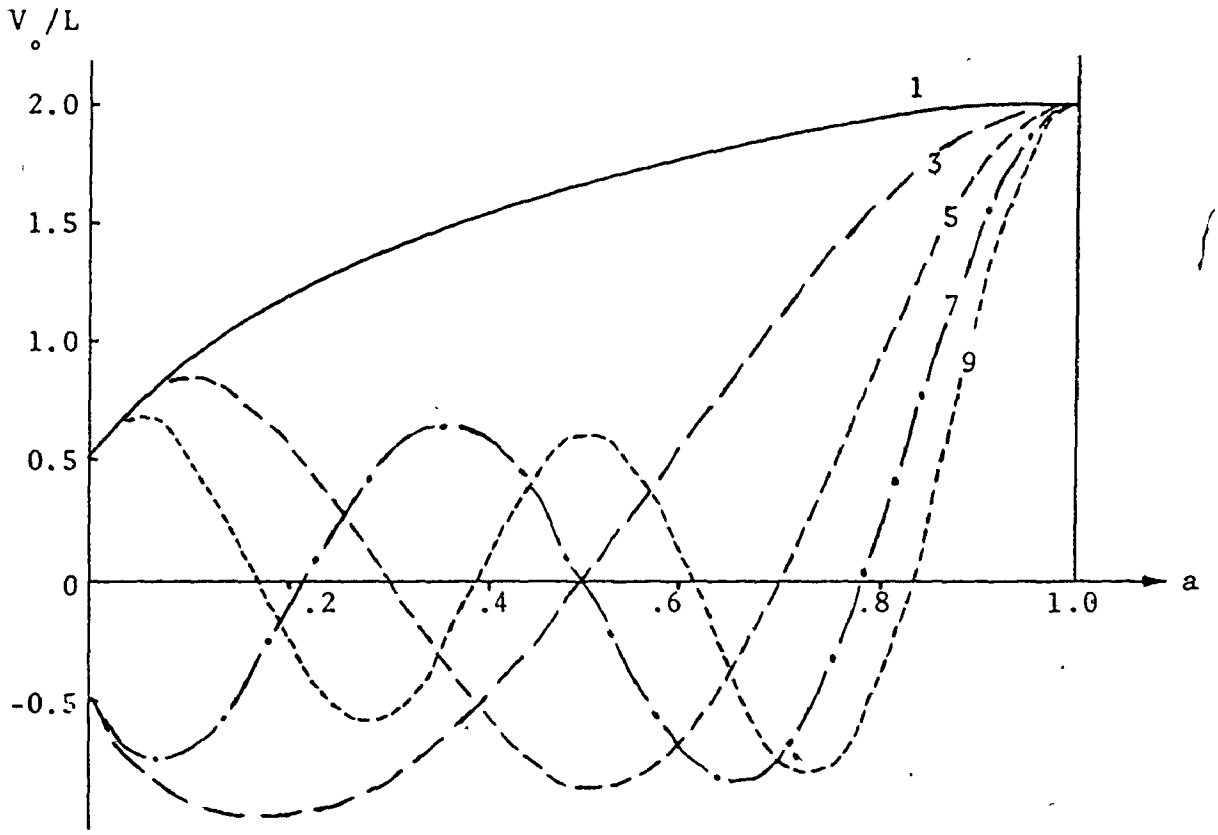

Figure 1.7 Amplitudes of Five Lowest Space Harmonics as Functions of a, where a = d/L

configurations regarding edge reflections also hold at the harmonic frequencies. The desired harmonic frequency is selected without the use of external filtering. The harmonic responses of both the input and output transducers are chosen such that all unwanted harmonics cancel, leaving only the desired response. Figure 1.8 demonstrates this method using a 4 finger or double-electrode structure for the input transducer and a three-finger structure for the output since these configurations both have slightly differing harmonic responses. A 1-GHz oscillator has successfully been implemented in [9] using this approach.

Another type of SAW oscillator is based on a relatively new device known as a SAW resonator. The SAW resonator is a one or two port device which can be implemented in a variety of different ways as shown in Figure 1.9. The resonator structure in each case consists of a resonant cavity set-up in the area between two sets of reflection gratings. The frequency of resonance is determined only by the finger periodicity, provided the width-to-gap ratio is unity. Theoretically at the resonant frequency, all of the acoustic energy radiated from the bi-directional transducer is reflected back which yields zero power dissipation and hence infinite impedance at that frequency. Since the behaviour of these resonators is analogous to bulk wave resonators, both have the same equivalent circuits. Resonator Q's in the order of 10,000 have been demonstrated. [11]. Encouraging results have also been obtained using grooved reflectors as opposed to the overlaid type. [12]. When the SAW resonator is inserted in the feedback loop of an amplifier, oscillations occur at the resonant frequency. This type of oscillator has many advantages over conventional types which are discussed in detail in [13].

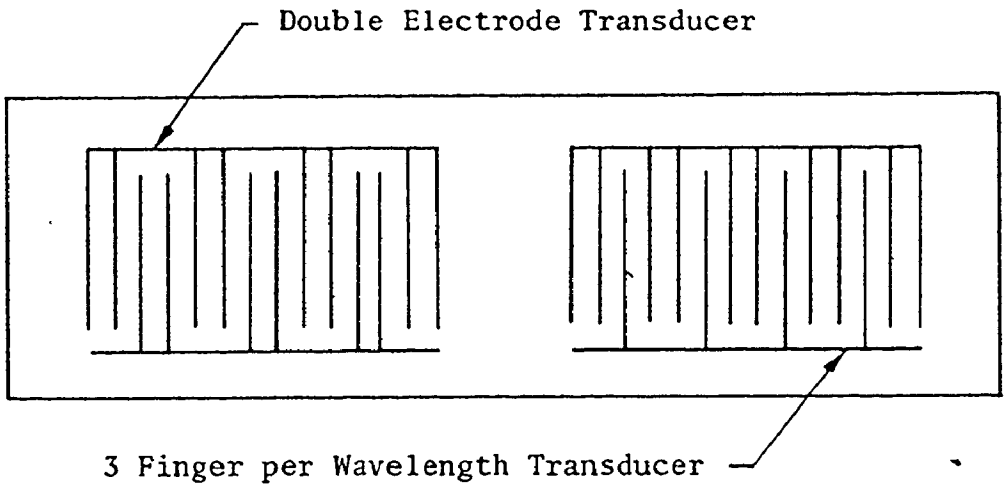

Figure 1.8 Single Harmonic Response Transducer Configuration

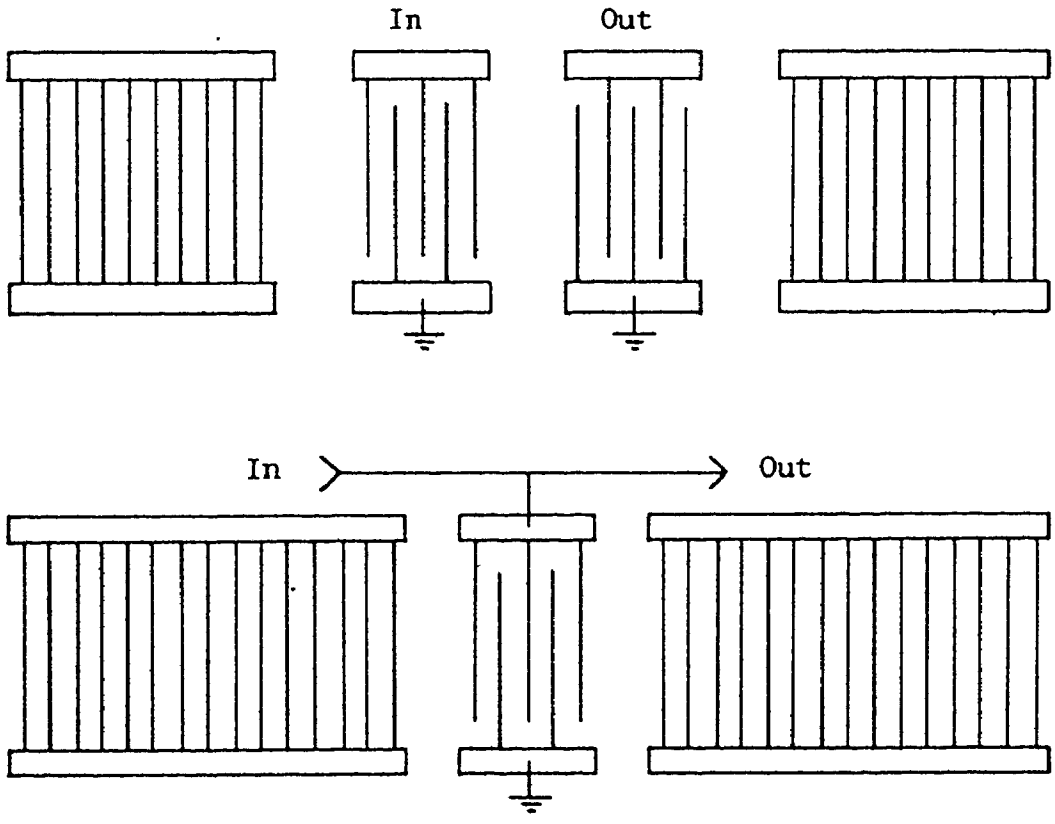

Figure 1.9 Various Geometries for SAW Resonators

CHAPTER II

THE DELAY LINE SAW OSCILLATOR

2.1 General

The prime frequency and stability determining element of the delay line SAW oscillator is the acoustic delay line. A rigorous derivation of delay line response along with the method of mode selection will be covered in this Chapter. Problems encountered in SAW design such as bulk mode coupling, triple-transit echo and electrical feedthru will also be covered. Amplifier design will only briefly be mentioned since this is secondary to the thesis topic. Finally, the integration of the SAW delay line with the amplifier will be discussed with emphasis on stability and matching considerations.

2.2 Theory of SAW Delay Line

The Fourier transform method of determining the frequency response of interdigital transducers is presently the most widely used and accepted. However, the IDT is a digitally-oriented device as the name implies since each period of an acoustic sinusoid is represented by two consecutive fingers on the transducer. Because of this digital representation, a form of analysis used in digital systems known as the Z-transform will be used to analyze the SAW delay line. The application of the Z-transform method to SAW analysis was derived by Dr. V.M. Ristic of the University of Toronto although this concept is mentioned earlier in [14].

The array of lines in Figure 2.1 represent the fingers of a SAW transducer equally spaced a distance d apart. The transfer function of

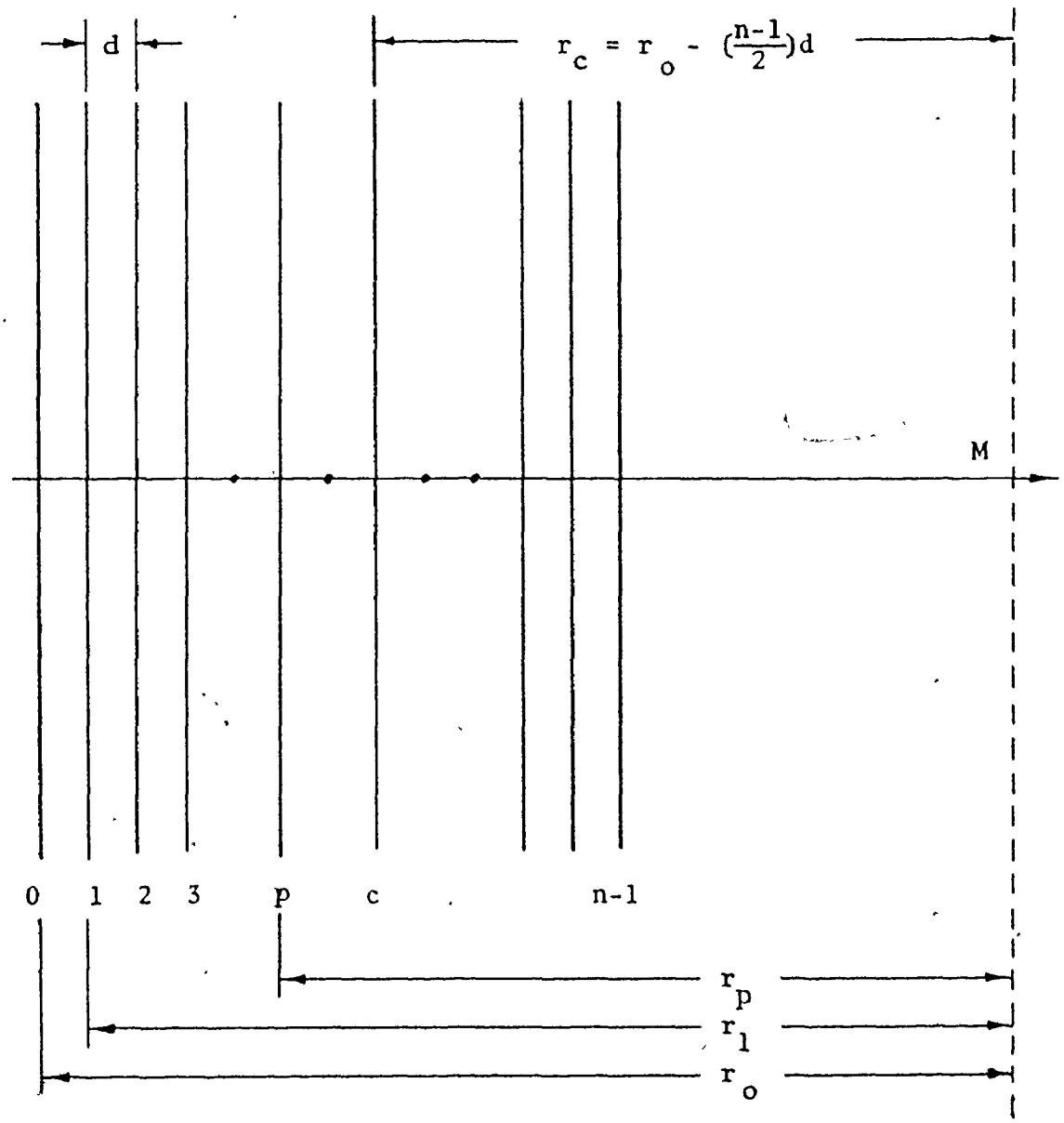

Figure 2.1 Array of Line Sources Representing a SAW Transducer

this array using the one-sided Z-transform can be expressed as:

$$E(z) = a_o + a_1 z^{-1} + ... + a_p z^{-p} + ... + a_{n-1} z^{-(n-1)}$$

$$= \sum_{p=0}^{n-1} a_p z^{-p} \qquad (2.1)$$

where $z = e^{j\alpha}$

$\alpha = \psi - kd$

n = number of fingers

The a_p are the weighting coefficients which in terms of a SAW transducer would represent the apodization coefficients. ψ is the phase difference between consecutive fingers in radians while d is the distance in meters between fingers. If the length of the fingers is many times greater than the wavelength of the frequency being considered, then the acoustic propagation can be considered dispersionless, in which case the wave vector k is equal to:

$$k = \frac{2\pi f}{v_a}$$

where f = input frequency

v_a = acoustic surface wave velocity

In the case of a uniform interdigital transducer used in SAW delay lines, the fingers are all the same length and therefore the sum becomes:

$$E(z) = G \sum_{p=0}^{n-1} z^{-p} \tag{2.2}$$

G is a constant and will be set to 1 for convenience since it does not alter the frequency response. Equation (2.1) then becomes:

$$\begin{aligned} E(z) &= \sum_{p=0}^{n-1} z^{-p} \\ &= \frac{1 - z^{-n}}{1 - z^{-1}} \end{aligned} \tag{2.3}$$

Substituting for z we get:

$$\begin{aligned} E(e^{j\alpha}) &= \frac{1 - e^{-j\alpha n}}{1 - e^{-j\alpha}} \\ &= \frac{\sin (n\,\alpha/2)}{\sin (\alpha/2)}\; e^{-j\alpha\frac{(n-1)}{2}} \end{aligned} \tag{2.4}$$

Equation (2.4) gives the response of the array at an observation point M and the phase term is derived from the phase centre of the array,

$$\psi_c = \left(\frac{n-1}{2} \right) \psi \tag{2.5}$$

Since a delay line also involves an output transducer, the inverse problem of calculating the response induced in an output array from a line source at observation point P is shown in Figure 2.2.

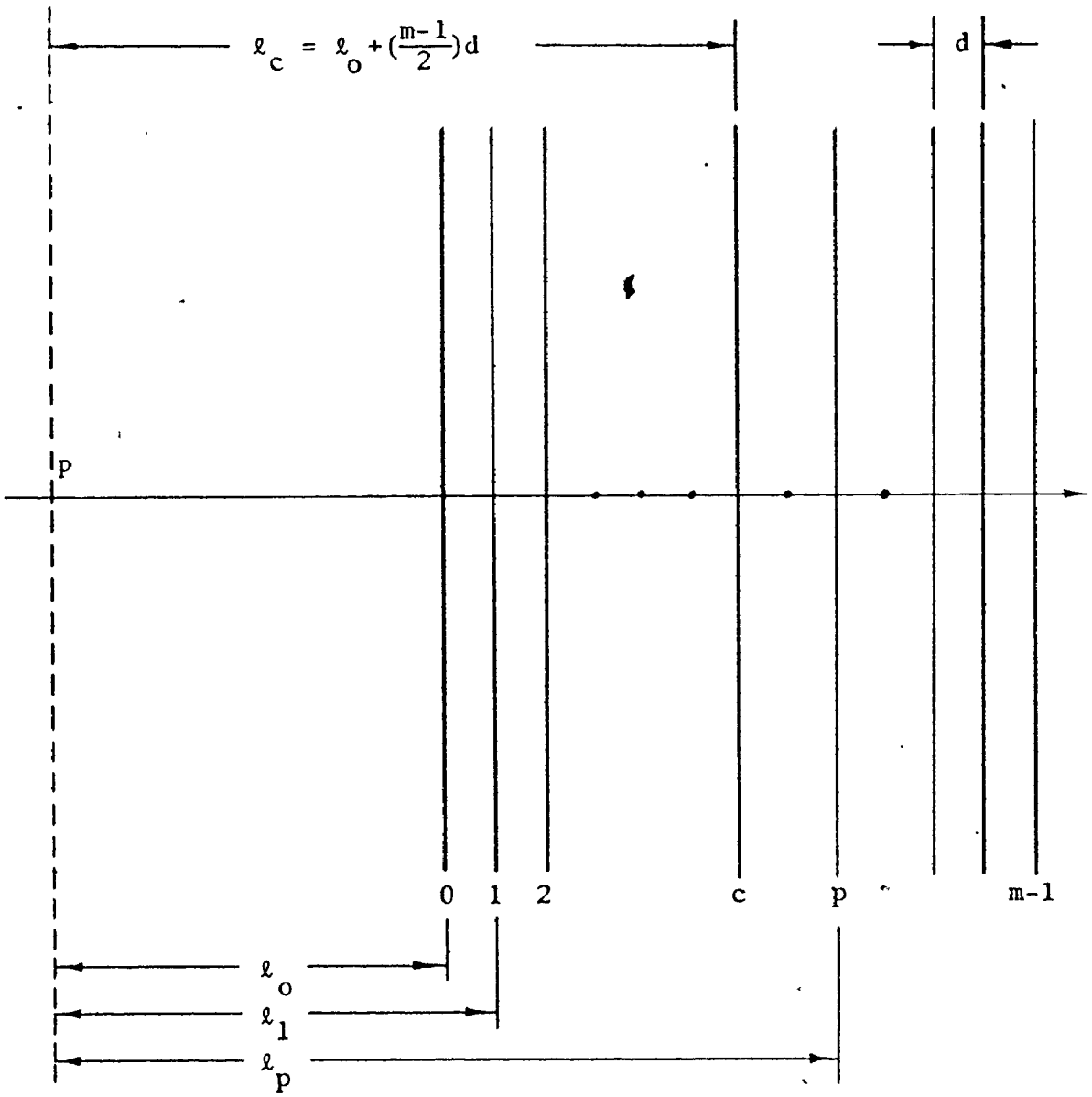

Figure 2.2 Array of Output Lines with Source at P

The total response of the array can be expressed as the sum of the individual responses of each finger. By use of the Z-transform this becomes:

$$E'(z) = b_o + b_1 z^1 + \ldots + b_q z^q + \ldots + b_m z^{(m-1)}$$

$$= \sum_{q=0}^{m-1} b_q z^q \qquad (2.6)$$

where $z = e^{j\alpha'}$

b_q = apodization coefficients

m = number of fingers (output array)

$\alpha' = -\alpha = kd - \psi$

It is assumed that the output array has the same finger spacing d as the input. Note that the sign of the phase term is reversed for the output array response. If the output array is uniform, equation (2.6) becomes:

$$E'(z) = \sum_{q=0}^{m-1} z^q \qquad (2.7)$$

$$= \frac{1 - z^m}{1 - z}$$

The combined response of the array system is simply the product of the input and output responses. Assume for simplicity that the number of fingers in both arrays is equal, that is, $n = m$. Then equation (2.7) becomes:

$$E'(z) = \frac{1 - z^{n}}{1 - z}$$

$$= E(z^{-1}) \tag{2.8}$$

Hence the total response is:

$$E(z)\ E'(z) = E(z)\ E(z^{-1})$$

$$= \left(\frac{1 - z^{-n}}{1 - z^{-1}}\right)\ \left(\frac{1 - z^{n}}{1 - z}\right)$$

$$= \frac{2 - (z^{n} + z^{-n})}{2 - (z + z^{-1})} \tag{2.9}$$

Substituting $z = e^{j\alpha}$ one obtains:

$$\left|E(e^{j\alpha})\right|^{2} = \left|\frac{\sin\ (n\ \frac{\alpha}{2})}{\sin\ (\frac{\alpha}{2})}\right|^{2} \tag{2.10}$$

The above equation represents the output response of two linear arrays. If the arrays are now connected as SAW transducers as shown in Figure 2.3 with an rf generating voltage exciting the input transducer, then the spacing d becomes:

$$d = \frac{\lambda_{o}}{2}$$

where $\lambda_{o} = \frac{v_{a}}{f_{o}}$ is the acoustic wavelength of the centre frequency of operation.

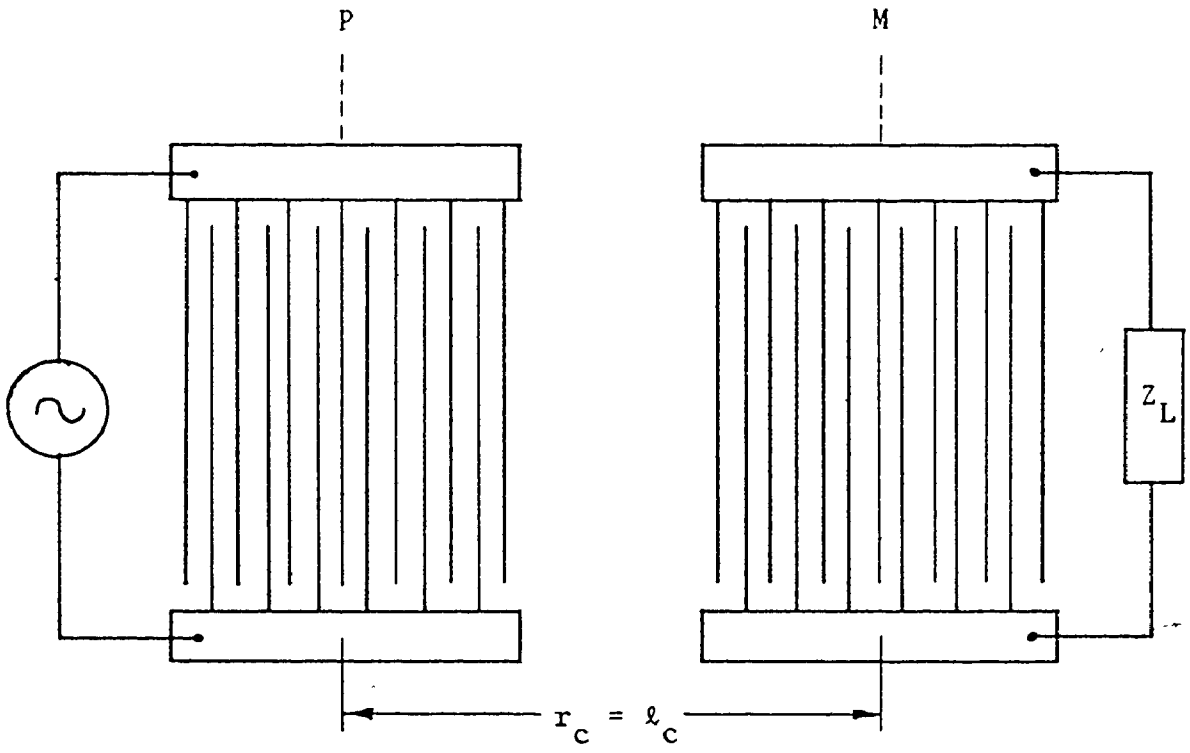

Figure 2.3 Linear Array Connected as SAW Transducer

Therefore the phase change ψ between adjacent fingers becomes π for a finger width-to-gap ratio of 1.

Hence α becomes:

$$\begin{aligned}\alpha &= \psi - kd \\ &= \pi - \left(\frac{2\pi f}{v_a}\right)\left(\frac{\lambda_o}{2}\right) \\ &= \pi\left(1 - \frac{f}{f_o}\right)\end{aligned}$$

Substituting the above in equation (2.10) yields:

$$|E(e^{j\alpha})|^2 = \left| \frac{\sin\left[\frac{n\pi}{2}\left(1 - \frac{f}{f_o}\right)\right]}{\sin\left[\frac{\pi}{2}\left(1 - \frac{f}{f_o}\right)\right]} \right|^2 \qquad (2.11)$$

Equation (2.11) is the output response of a SAW delay line with n fingers in each transducer. A computer plot of the output for n = 100 and f_o = 100 MHz is shown in Figure 2.4. The response clearly demonstrates the bandpass characteristic exhibited by a simple SAW delay line. The time delay for these devices is calculated between the phase centres of the input and output transducers and is given by:

$$t_d = \frac{\ell_c}{v_a} \qquad (2.12)$$

where ℓ_c = distance between transducer centres

The time delay is independent of frequency and depends only on the acoustic surface wave velocity associated with the substrate, and the spacing between the transducers.

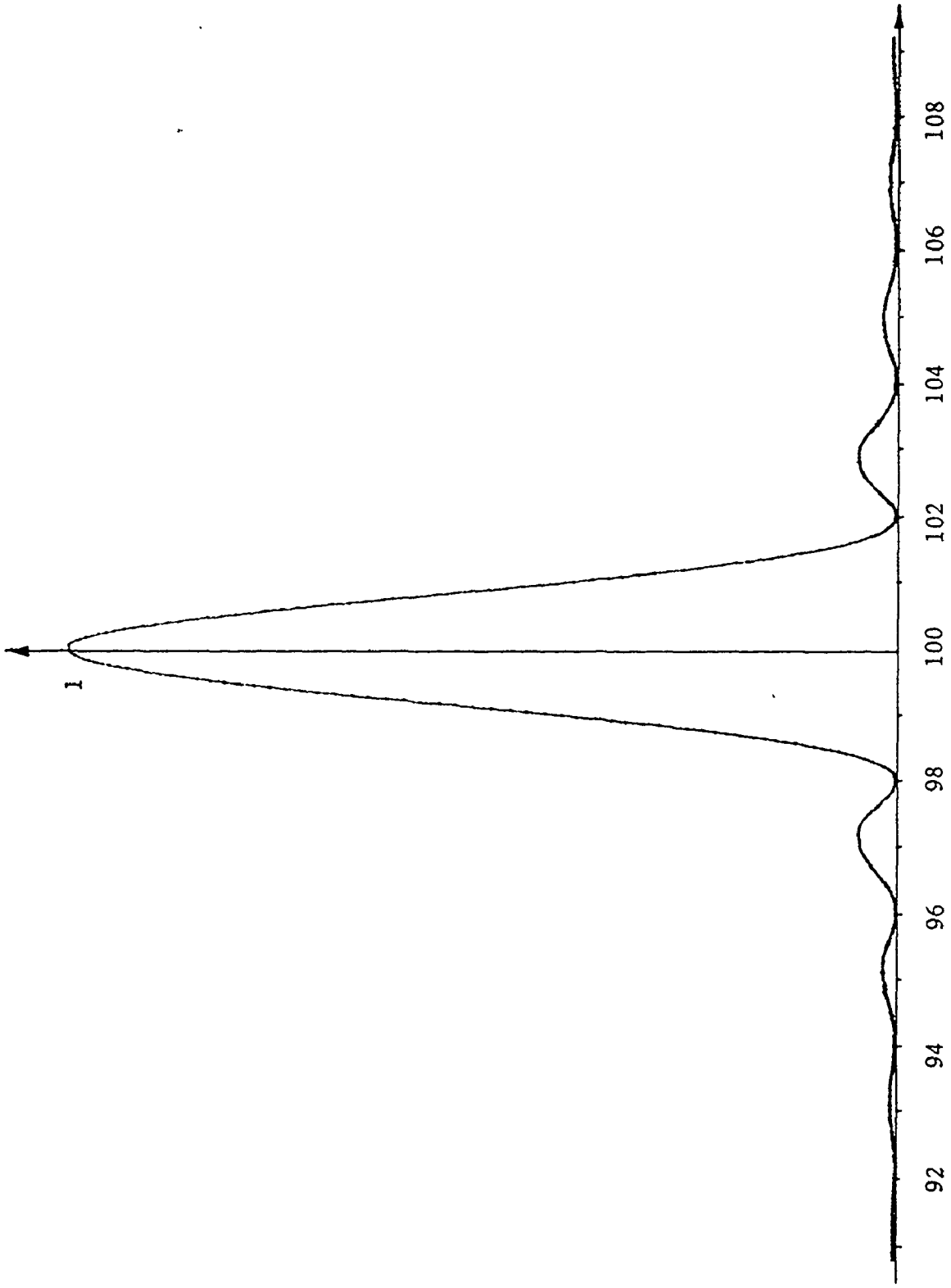

Figure 2.4 Computer Plot of SAW Delay Line Frequency Response (Normalized)

2.3 Mode Selection

Having calculated the frequency response of the SAW delay line it is necessary to consider the frequency mode selection for the oscillator. Figure 2.5 shows the feedback loop of the SAW oscillator. This loop can support a comb of frequencies for which the net phase shift around the loop is $2p\pi$, where p is an integer, hence:

$$\frac{2\pi f_A \ell}{v_a} + \phi_E = 2p\pi \qquad (2.13)$$

where ℓ = distance between phase centres of arrays

ϕ_E = electrical phase shift in amplifier

The phase shift due to the amplifier is usually $\leq 2\pi$ while the acoustic phase shift $\frac{\omega\ell}{v_a}$ may be of the order of 200π. Therefore, neglecting ϕ_E, the allowed oscillation frequencies are:

$$f_A \simeq \frac{pv_a}{\ell} \qquad (2.14)$$

In order to select one frequency f_o, the delay line transducers are both centred on f_o and the delay path-length ℓ is made equal to the length of the large transducer in Figure 2.5. [15]. The frequency selectivity is provided primarily by the larger input transducer since it has a narrower bandpass response because of its many fingers. Since ℓ is made equal to the length of the input transducer, the output transducer must physically be shorter to avoid problems arising from close proximity. The output transducer therefore has a wider bandpass response and consequently plays a minor role in the frequency selectivity of the system.

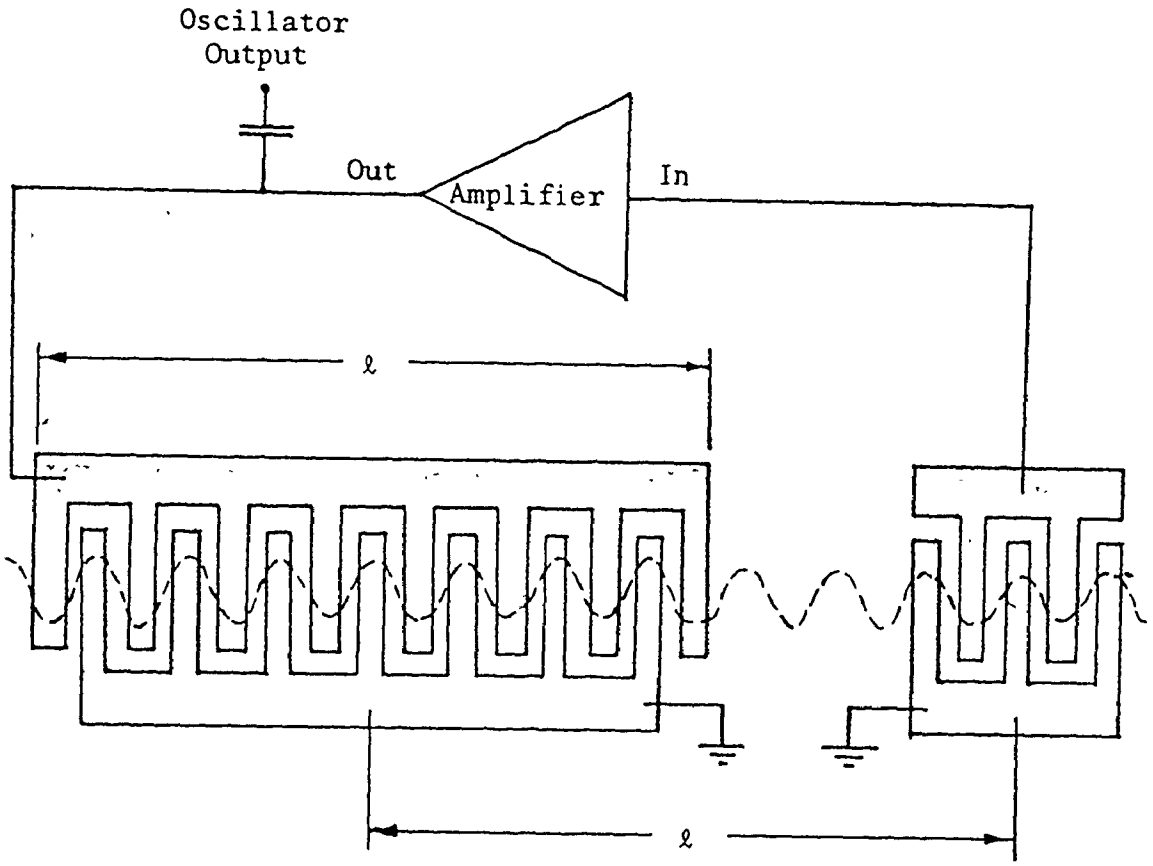

Figure 2.5 SAW Oscillator Delay Line Feedback Loop

The mode selection is based on the principle that the nodes of the frequency response of the large input transducer occur where the other possible oscillation frequencies are situated and hence f_o is the only frequency which is not suppressed. For frequencies close to f_o, equation (2.11) can be approximated as follows:

$$E(x)^2 = \left(\frac{n \sin x}{x} \right)^2 \qquad (2.15)$$

where $$x = \frac{n\pi}{2} \left(1 - \frac{f}{f_o} \right)$$

The above equation has nodes for $x = m\pi$, m an integer $\neq 0$, therefore:

$$m\pi = \frac{n\pi}{2} \left(1 - \frac{f}{f_o} \right)$$

$$f = f_o \left(1 - \frac{2m}{n} \right) \qquad (2.16)$$

Let $N = n/2$ be the number of finger pairs in the transducer, then (2.16) becomes:

$$f = f_o \left(1 - \frac{m}{N} \right) \qquad m \neq 0 \qquad (2.17)$$

This equation implies that the distance between the nodes (of the sidelobes) of the transducer frequency response is f_o/N as shown in Figure 2.6. If $\ell = N\lambda_o$, the length of the input transducer, then equation

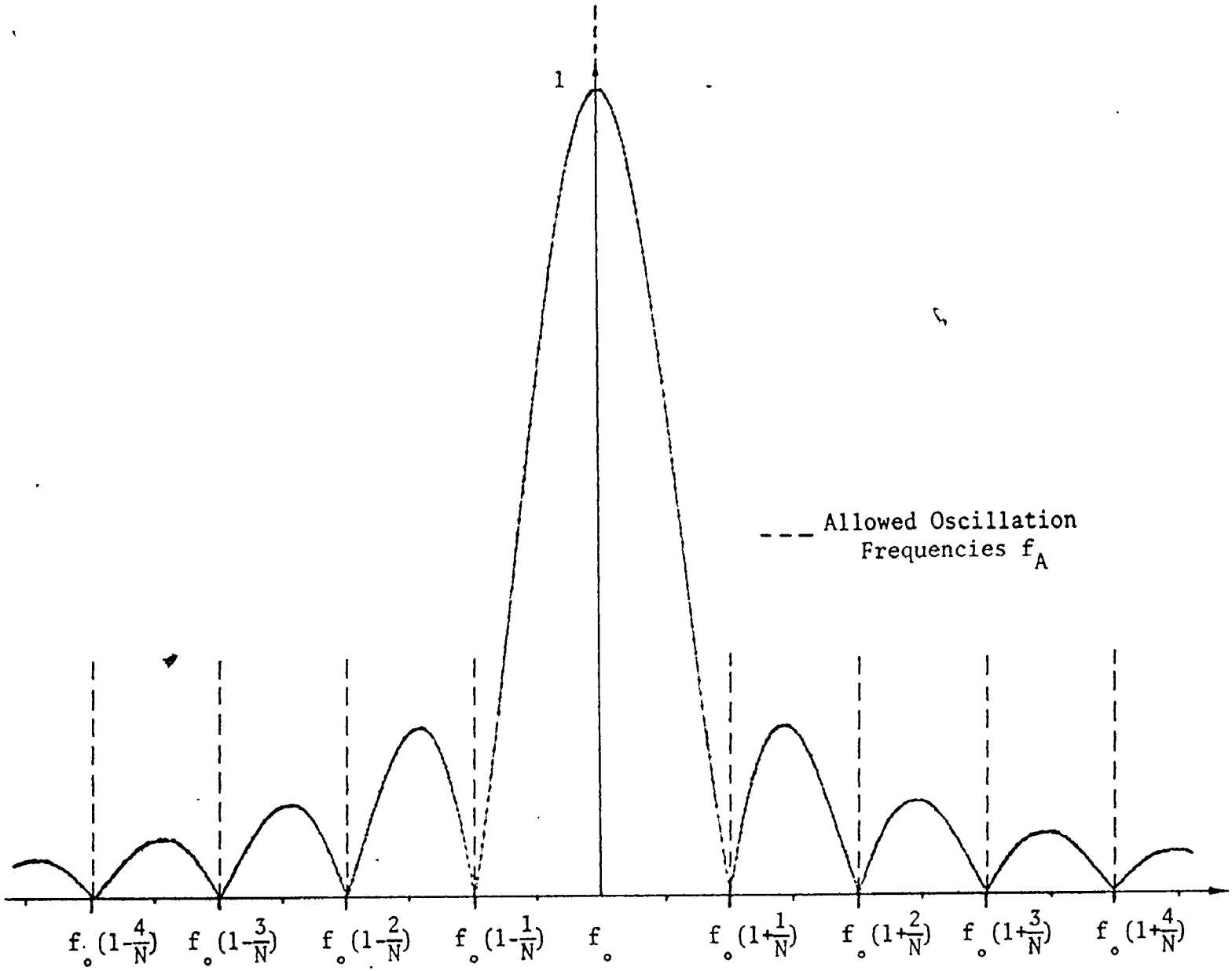

Figure 2.6 Response of Input Transducer Showing Mode Selection Characteristics (Normalized)

(2.14) becomes:

$$f_A = \frac{pf_o\lambda_o}{N\lambda_o} = \frac{pf_o}{N} \qquad (2.18)$$

Comparing equations (2.17) and (2.18), all of the allowable frequencie of oscillation except f_o occur at the nodes of the transducer response and are therefore suppressed to prevent mode ambiguity.

2.4 Problems Encountered in SAW Design

After the filter synthesis is complete, consideration must be given to the possible secondary effects and spurious responses occuring in the device which have to be suppressed. These effects are shown in Figure 2.7. With the small dimensions and close tolerances of SAW devices, direct electrical feedthru can become a problem. This can be avoided by careful design of the substrate package and by keeping lead lengths short and the capacitance to ground at a minimum. Electrical feedthru can also be suppressed quite effectively by feeding the input and output transducers at opposite ends (Figure 2.8) as reported in [16] and later in [3].

Bulk acoustic modes can also be generated by the launching of surface waves. These modes affect the frequency response above the passband by causing distortions as shown in Figure 2.9. The bulk waves are usually generated at some angle ϕ from the surface into the substrate. In terms of linear array theory this is comparable to energy being radiated in the side lobes which is then mode-converted to bulk waves in the SAW

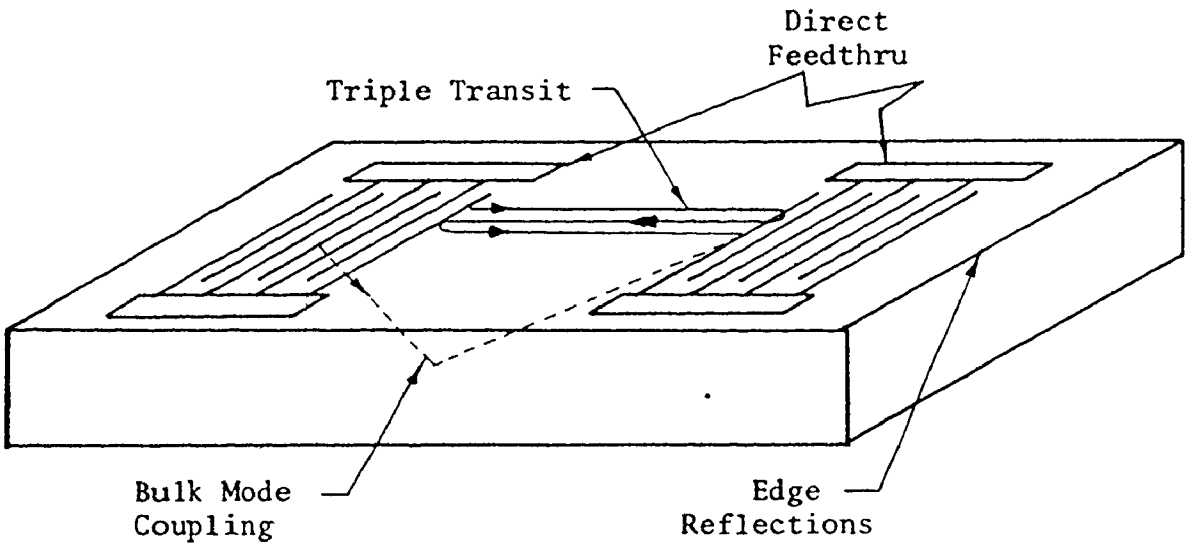

Figure 2.7 Problems Encountered with a SAW Delay Line

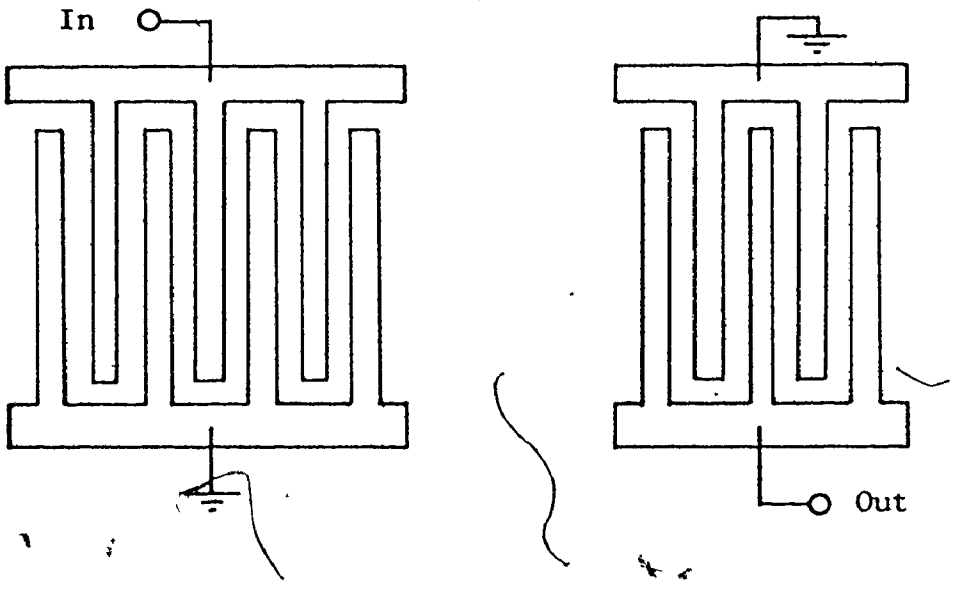

Figure 2.8 Method of Termination to Suppress Electrical Feedthru

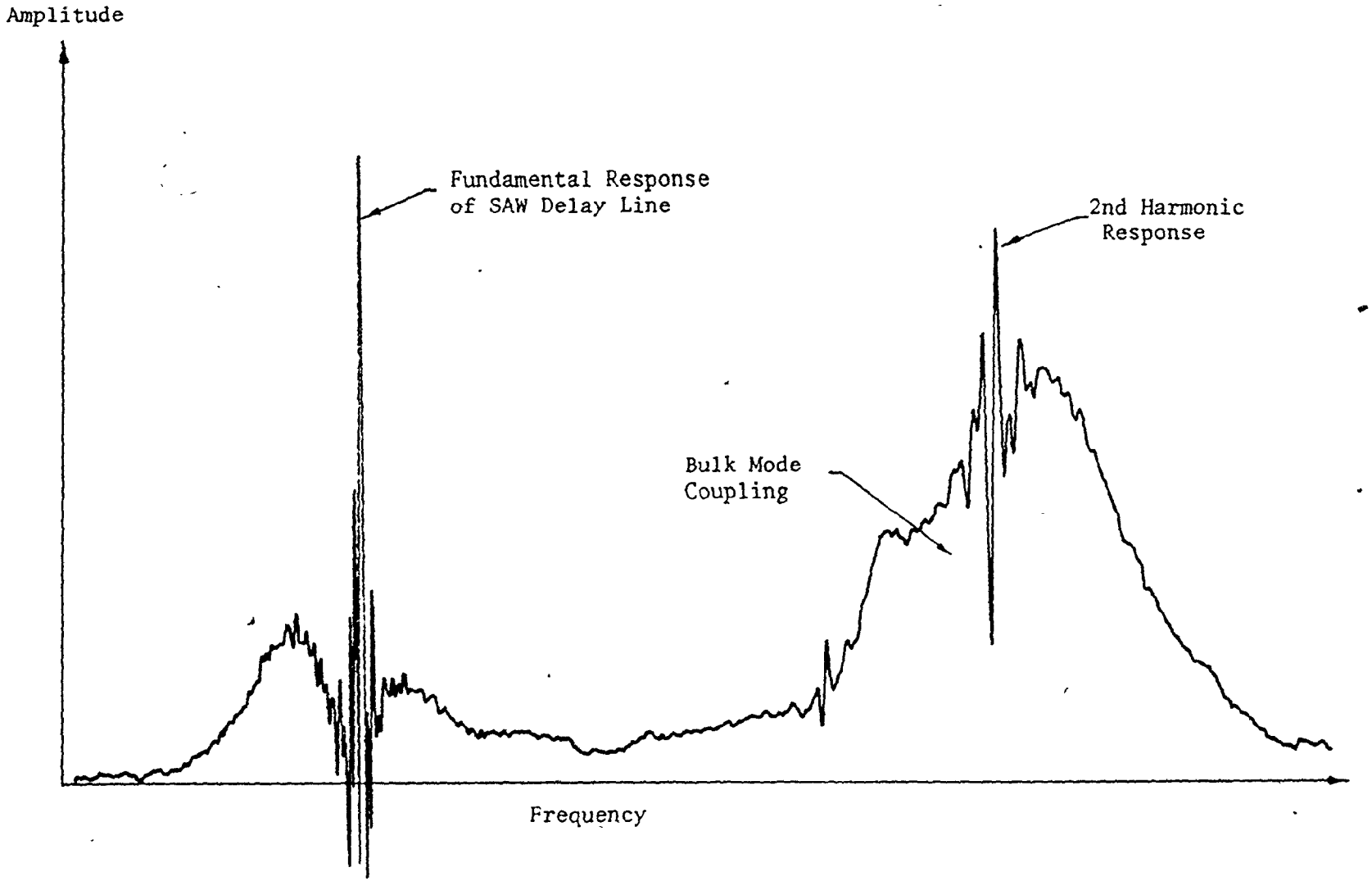

Figure 2.9 Swept Frequency Response of a SAW Delay Line
Showing Bulk Mode Interference

substrate. As the number of fingers increase, the side lobe levels decrease and hence there is less coupling to bulk waves. Since these bulk waves are generated at an angle ϕ to the surface, they are reflected from the bottom surface of the substrate and excite the output transducer to produce distortions in the response. One method of alleviating the problem of bulk wave interference is to have a roughened lower substrate surface which will scatter any incident bulk waves, thereby decreasing their effect on the output transducer. A more involved solution to the problem consists of machining a transverse bevel on the lower surface of the substrate which would reflect the bulk waves off to the sides of the substrate rather than to the surface again. [17]

Propagation losses must also be considered in the design of SAW devices although this problem only becomes serious at higher frequencies of 1 GHz and up. At 1 GHz there is a propagation loss associated with the substrate of a few dB per μsec. and this loss increases as f_o^2 for higher frequencies. [18]. At lower frequencies these losses due to the substrate are negligible, however other losses occur due to finger resistance and mass loading. The conducting layer of a transducer finger must be thick enough to prevent excessive ohmic losses and yet it must be thin enough to prevent mass loading of the acoustic wave.

Other losses can also be caused by diffraction and beam steering. Diffraction is considered a fixed physical phenomena due to the substrate material [19] although the presence of fingers on a surface can cause a change in surface wave velocity which disperses the wave. This problem only becomes serious at higher frequencies in the order of 1 GHz and above.

Beam steering is a function of exact transducer alignment with the crystallographic direction of propagation, and its effects depend upon the coupling and velocity profiles of the substrate material for various error angles θ from the true propagation direction. ST-X quartz, for example, varies only slightly in its velocity profile about the true X-direction of propagation and therefore transducer alignment is not as critical for this type of substrate. The combined effects of diffraction and beam steering are shown in Figure 2.10 [19] for ST-X quartz where it is seen that these losses increase as the distance between the input and output transducers increases.

Triple transit echo arises from finger reflections and the acoustic wave travels a total of three delay times before exciting the output transducer again. This undesirable response is measured by comparing the levels of the desired delayed signal and the first multiple echo. The effect is not as serious on high loss substrates or for transducers which are not matched to their electrical circuits. [17]. Triple transit echo can be suppressed by using the double-electrode structure for the transducers since edge reflections in this configuration cancel. The disadvantage of this method is the increased resolution requirements needed in the fabrication process. There are also other acoustic reflections from fingers and substrate edges which cause distortions in the passband response. The simple delay line configuration discussed earlier has a minimum insertion loss of 6 dB associated with it due to the bi-directionality of the simple transducers. The acoustic wave travelling away from the output transducer must be suppressed to prevent it from

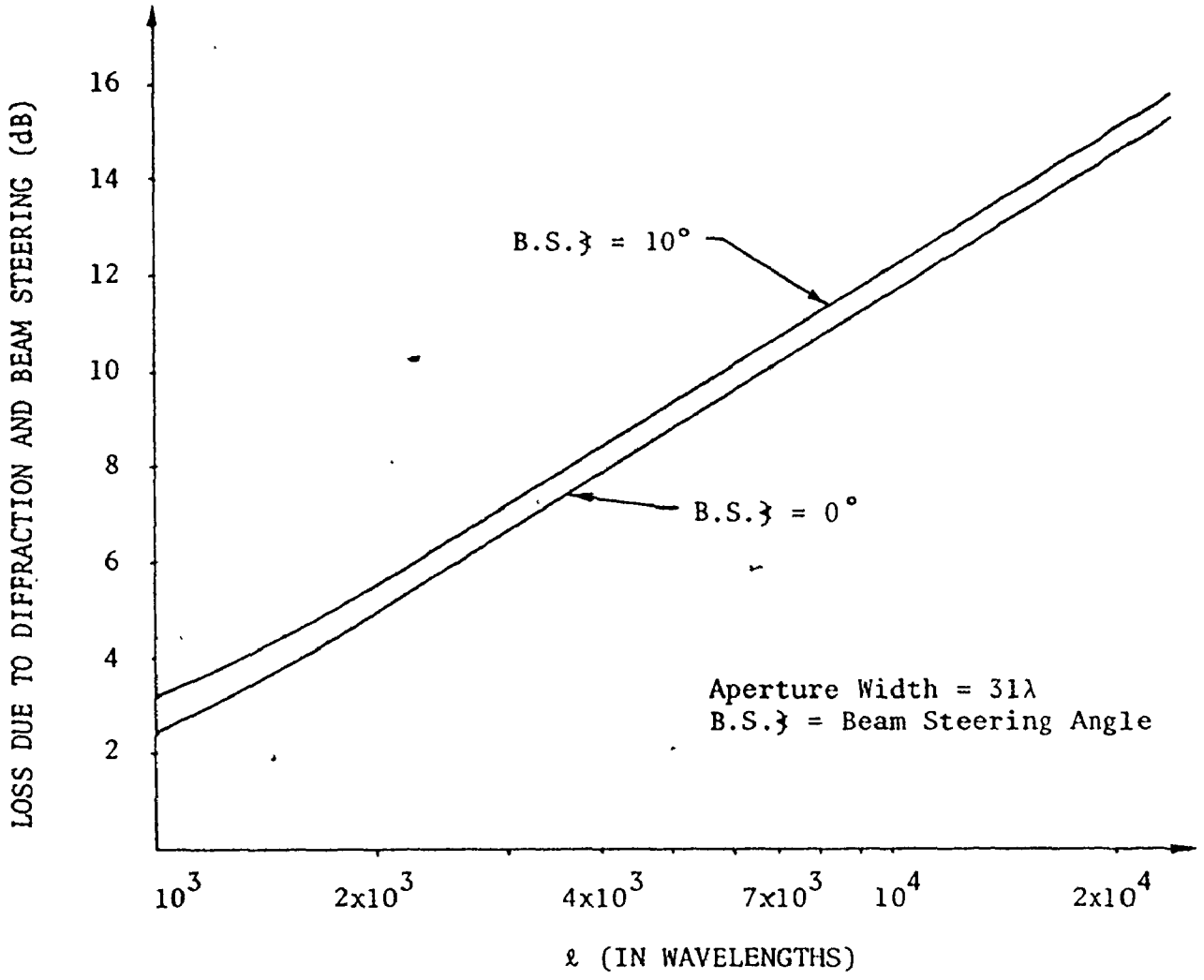

Figure 2.10 Combined Effects of Diffraction and Beam Steering for ST-X Quartz

being reflected back towards the transducers and thereby cause distortions. Acoustic absorbers are therefore used at the edges of the substrate on either side of the delay line to suppress these unused surface waves. Paraffin or vacuum grease is used to provide the acoustic absorption.

SAW device fabrication can sometimes present a problem which must be considered in the initial design of the device. There are numerous methods of lithography and fabrication techniques used in the area of SAW devices, each with their own peculiar problems and disadvantages. [20]. Photolithography in conjunction with chemical etching is the most common technique used for SAW devices in the low megahertz to 1 GHz region. Since the delay line in this thesis is in the low megahertz region, there are no major problems associated with its fabrication and therefore the problems associated with higher frequencies and other methods will not be discussed.

2.5 Matching and Amplifier Considerations

The delay line SAW oscillator will operate at maximum efficiency when the delay line is matched at input and output to the feedback amplifier. Consideration of the impedance seen by the oscillator output must also be accounted for. At maximum efficiency, the least amount of input power is needed for the amplifier to provide the necessary gain for oscillation to occur. The matching of delay lines is usually implemented with passive components such as coils or even active circuits. The common aperture widths and transducer sizes used in SAW devices yield impedances other than the characteristic impedance of the system, which is usually 50 Ω.

Hence passive or active matching networks are needed so that maximum power transfer can take place. Matching networks however are not very desirable for delay lines used in SAW oscillators. The components of the matching network are very temperature sensitive in most cases and the end result would be degradation of oscillator stability. The alternative is to design the input transducer such that the input reactive impedance is 50 Ω, which will yield a minimum untuned insertion loss. The output transducer reactive impedance will then automatically be higher for the same aperture width since the number of fingers are proportionally less than for the input transducer.

The equivalent circuit in Figure 2.11 (a) represents a many-fingered transducer near resonance on a low coupling factor substrate such as ST-X quartz. Figure 2.11 (b) shows the equivalent series circuit representation of a SAW transducer with fewer fingers on a low coupling factor substrate. C_T is the total capacitance and R_a is the radiation resistance of the transducer. The total capacitance can be calculated using the following formulas [21] assuming that the finger thickness is much less than the finger-to-finger spacing:

$$\epsilon_{PR}^{T} = \frac{1}{\epsilon_o} \left(\epsilon_{11}\, \epsilon_{33} - \epsilon_{13}^2 \right)^{1/2} \tag{2.19}$$

$$C_{FF} = 2\left(\epsilon_{PR}^{T} + 1\right) \left[6.5\left(\frac{d}{L}\right)^2 + 1.08\left(\frac{d}{L}\right) + 2.37 \right] \times 10^{-12} \tag{2.20}$$

$$C_T = C_{FF} \hat{L} N \lambda_o \tag{2.21}$$

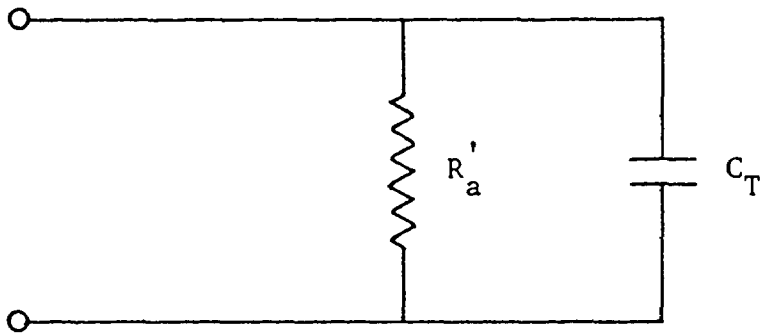

Figure 2.11 (a) Equivalent Circuit for a Many-Fingered Transducer Near Resonance on a Low -k^2 Substrate

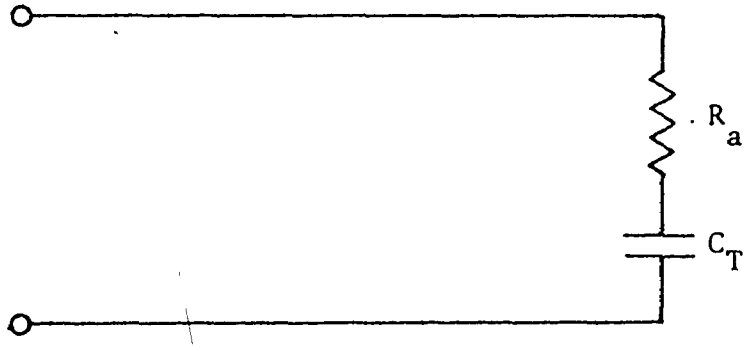

Figure 2.11 (b) Series Circuit Approximation

where d = finger width

L = centre-to-centre finger spacing

λ_o = acoustic wavelength of centre frequency

N = number of finger pairs in transducer

$\hat{L}$ = acoustic aperture in wavelengths

ε_o = permittivity of free space = 8.854×10^{-12} farad/m

$\varepsilon_{11}, \varepsilon_{33}, \varepsilon_{13}$ = dielectric constants of substrate

C_{FF} is the capacitance per unit length of a single period, that is, the capacitance between any two conducting fingers situated on a substrate with relative dielectric constant ε_{PR}^{T}, and with a finger width-to-gap ratio of unity. The dielectric constants of the piezoelectric substrate are taken at constant stress with the 1 direction being the direction of propagation. The radiation resistance R_a of the transducer can be thought of in terms of the radiation resistance of a linear array. The total power dissipated in the conversion to acoustic energy in a SAW transducer can be represented by the power dissipated in a resistance R_a. The approximate expression for R_a is [22]:

$$R_a = \frac{2Nk^2}{\pi^2 f_o C_T} \tag{2.22}$$

where k^2 is the coupling coefficient of the substrate material.

The impedance of the transducer from the series equivalent circuit is:

$$Z_o = R_a + \frac{1}{j\omega C_T} \tag{2.23}$$

For a 50 Ω system, $|Z_o|$ will equal 50 Ω and the transducer parameters can be adjusted accordingly for a proper impedance match. For a SAW oscillator delay line the centre frequency and number of fingers N_1 and N_2 for both transducers are already determined from the frequency response and mode selection specifications. Therefore the only parameter which can be varied to adjust the impedance is the aperture width $\hat{L}$. Since the aperture widths of both input and output transducers are the same, the reactive impedance of the output transducer with less fingers will be proportionally higher. However, this higher impedance can be matched to the input stage of the feedback amplifier simply by designing the amplifier such that its input impedance equals the reactive impedance of the output transducer.

The overall stability of the SAW oscillator depends on the substrate material and the amplifier. The frequency f of SAW oscillators varies with temperature T(°C) as [8]:

$$f \approx f_o \left[1 - 3 \times 10^{-8} (T - T_o)^2 \right] \qquad (2.24)$$

where f_o is the maximum frequency occuring at temperature T_o. Unless a thermostat is applied to the oscillator, changes in temperature will cause the frequency of oscillation to drift down as the temperature goes up. From the above equation, if the temperature is held at T_o within ±4°C then the resulting frequency deviation will be less than 1 ppm, which is quite respectable for a medium-term stability factor. Further aspects of substrate temperature stability will be covered in the next Chapter.

The stability of the amplifier also affects the frequency stability of the SAW oscillator. Changes in amplifier gain due to temperature variations or poor design will cause phase changes in the feedback loop. For optimum stability, a high-power low-noise amplifier should be used in conjunction with a low-loss SAW delay line. The amplifier can be designed for a wide bandpass characteristic with the delay line response situated at the centre. This would eliminate electrical feedthru and harmonics at higher frequencies from propagating around the loop and consequently wasting amplifier power. The general design of broadband amplifiers in the UHF frequency range is covered in [23]. If impedance matching is desired without altering the design of a commercially available 50 Ω amplifier, then simple wide-band toroidal transformers may be used. These transformers consist of twisted-wire-pair transmission lines wound on ferrite cores and are effective up to several hundred megahertz. [24]. The use of these matching transformers however would degrade the frequency stability characteristic of a SAW oscillator unless the temperature is controlled in an oven. A simple method of matching using strip-line techniques will be discussed in Chapter V which overcomes some of the temperature variation problems.

CHAPTER III

DESIGN AND FABRICATION OF 124 MHz SAW OSCILLATOR

3.1 General

The most important consideration in the design of the SAW oscillator is the choice of the substrate. All further considerations such as transducer design and oscillator stability depend heavily on the choice of the substrate. One substrate in particular is the most suitable for oscillator applications and the reasons for this choice will be discussed in the first part of this chapter. Transducer design will be covered using the design criteria presented in the last Chapter. Finally the delay line fabrication procedure will be covered in detail along with its integration with an amplifier.

3.2 Substrate Considerations

The two most commonly used substrate materials for SAW devices are lithium niobate ($LiNbO_3$) and quartz. The general properties of these materials are shown in Figure 3.1. [21]. The temperature coefficient of velocity for each of the $LiNbO_3$ materials is seen to be appreciably higher than for the quartz materials. The other major difference between these two types of materials is the coupling coefficient k^2 which is a measure of the efficiency with which electrical energy can be converted into mechanical energy on a piezoelectric surface. This is expressed in terms of the material properties (dielectric constants) and $\Delta v_a/v_a$,

Material	Orientation	v_a m/s	$\frac{\Delta v_a}{v_\infty}$	k^2 (measured)	Temperature Coeff. of Delay ppm/°C	C_{FF} in F/m for $\frac{d}{L} = 0.5$	Attenuation at 1 GHz dB/μsec in Air	ε_{PR}^T
$LiNbO_3$	Y,Z	3488	0.0241	0.045	85	4.6438×10^{-10}	0.88	50.2
$LiNbO_3$	41.5°X	4000	0.028	0.057	67	6.1857×10^{-10}	0.75	67.2
Quartz	Y,X	3159	0.0009	0.0023	-24	5.00664×10^{-11}	2.15	4.52
Quartz	ST,X (Y+42 3/4°,X)	3158	0.0006	0.0016	0	5.03385×10^{-11}	2.62	4.55

Figure 3.1 Characteristics of Various Substrate Materials [5], [21]

the fractional change in SAW velocity when a thin, massless conductor is deposited on the propagation surface: [25]

$$k^2 = 2(1 + 1/\epsilon_{PR}^T) \frac{\Delta v_a}{v_a} (1 - \frac{\Delta v_a}{v_a}) \qquad (3.1)$$

where ϵ_{PR}^T has been defined in Equation (2.19).

The primary consideration in choosing a substrate material for oscillator delay line applications is temperature stability. Based on this premise, ST-X quartz is the most suitable choice since it has a first-order temperature coefficient of 0 ppm/°C. This characteristic arises from the special cut of quartz known as the rotated Y-cut at 42 3/4° with propagation along the X-axis as shown in Figure 3.2. [22]. For all rotated Y-cuts, the surface acoustic wave velocity and its temperature dependence are at a maximum when the propagation is in the X-direction. The second-order coefficient of phase delay change was experimentally determined in [22] to be approximately 31.5 x $10^{-9}/°C^2$. This result has recently been confirmed in [26]. Figure 3.3 shows these results where various cut angles of alpha quartz are tested for their temperature dependence and the first, second and third order coefficients of the least squares fit are listed. The actual time delay between two transducers on alpha quartz is given by:

$$\tau = t_{25}[1 + A(T - 25) + B(T - 25)^2 + C(T - 25)^3] \qquad (3.2)$$

where T = operating temperature in °C

t_{25} = time delay between two transducers at 25°C

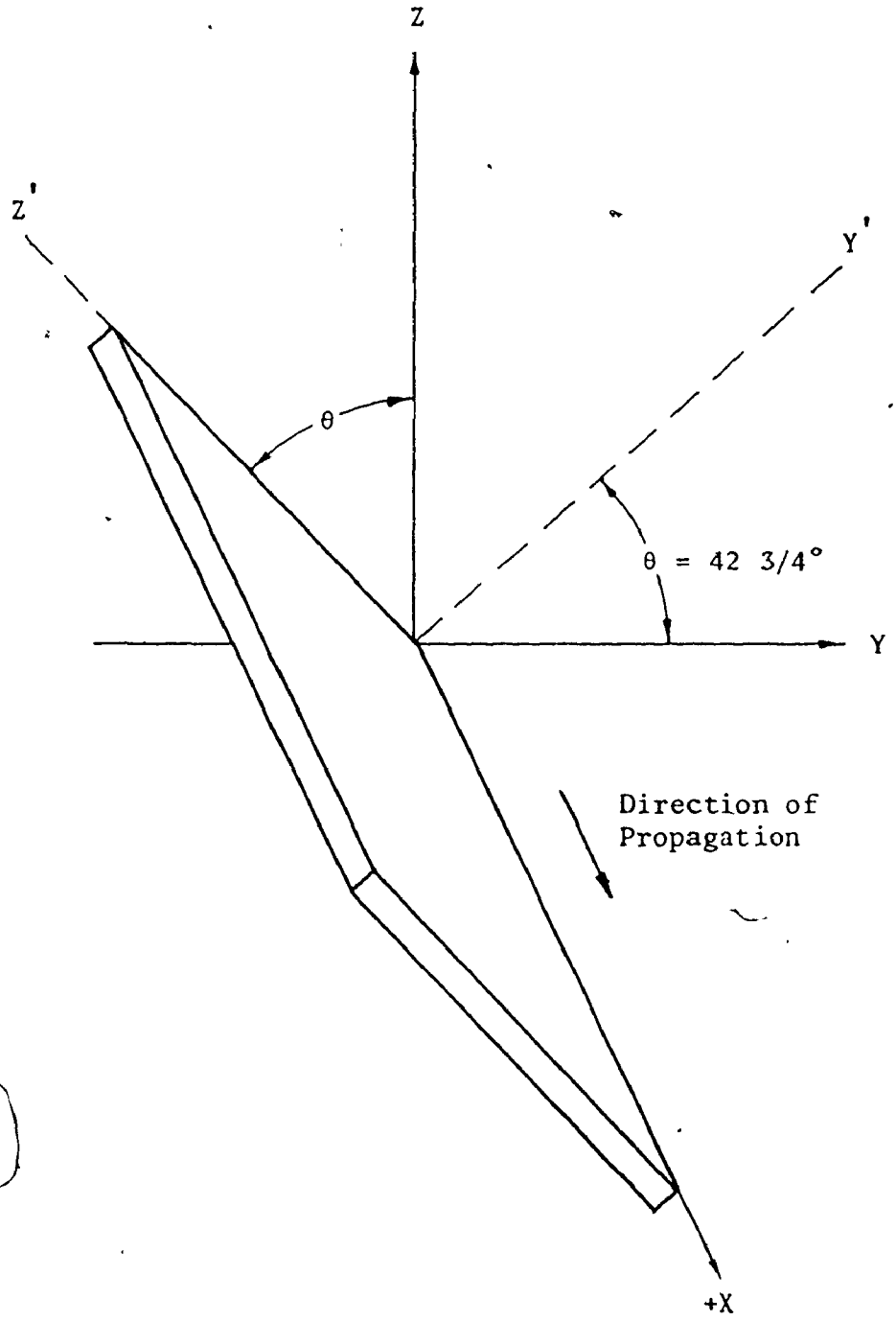

Figure 3.2 ST-Cut of Quartz Shown Relative to Crystal Axes

The A, B, and C coefficients are as given in Figure 3.3, depending on the cut angle θ. The overall temperature dependence of the phase-delay-change for ST-X quartz (θ = 42 3/4°) is shown in Figure 3.4. The zero slope point of this curve was found in [9] to shift as a function of frequency and the percent of the acoustic path which was metallized. As the metallization ratio and frequency increase, the zero slope point of the phase-delay-change curve shifts downward in temperature. This problem becomes serious only when higher metallization ratios are used in conjunction with very long transducers and does not seriously affect the design of the SAW oscillator in this thesis.

There are also other advantages in the choice of ST-X quartz for oscillator applications. For small bandwidths (less than 5%) quartz is less susceptible to reflections and second-order perturbations, and also exhibits superior triple-transit suppression compared to $LiNbO_3$. The major disadvantage is the larger insertion loss associated with quartz due to the much smaller coupling coefficient k^2. In the low megahertz to 1 GHz range this inherent insertion loss can be tolerated and compensated for with the use of proper matching and low noise amplification.

The amplitude and phase error characteristics for ST-X quartz are shown as a function of transducer aperture width $\hat{L}$ and centre-to-centre spacing ℓ_c between transducers in Figure 3.5. [14]. Since SAW oscillator delay lines usually have wide aperture widths comparable to the distance between transducer centres, then amplitude and phase errors will be negligible. Figure 3.6 [14] shows the SAW reflections as a function of the number of electrodes in the transducer for several common substrate materials. ST-X quartz exhibits the least reflection loss

ANGLE OF ROTATION θ°	TURNOVER TEMPERATURE °C (ZERO SLOPE)	FIRST ORDER COEFFICIENT A $X10^{-6}/(°C)$	SECOND ORDER COEFFICIENT B $X10^{-9}/(°C)^2$	THIRD ORDER COEFFICIENT C $X10^{-12}/(°C)^3$
35	83.5	-3.65	+35.9 (26.4)	-54.0
37	65.8	-2.47	+34.5 (26.1)	-68.0
40	40.0	-0.91	+30.3 (30.1)	- 3.0
42.75	21.1	+0.25	+32.3 (32.0)	+18.0
42.25	-5.9	+2.26	+38.8 (34.6)	+46.0
33.09	114.3	-4.99	+31.6 (24.3)	-27.0
34.17	99.8	-4.51	+34.1 (26.3)	-35.0
36.11	78.5	-3.00	+26.8 (29.4)	+16.0
37.14	65.9	-2.36	+29.9 (27.8)	-17.0
38.37	50.6	-1.66	+32.2 (32.4)	+ 3.0

Figure 3.3 Turnover Temperature and Coefficients of Delay Time for Several Rotated Y-Cuts of Alpha Quartz (Normalized to 25°C) [26]

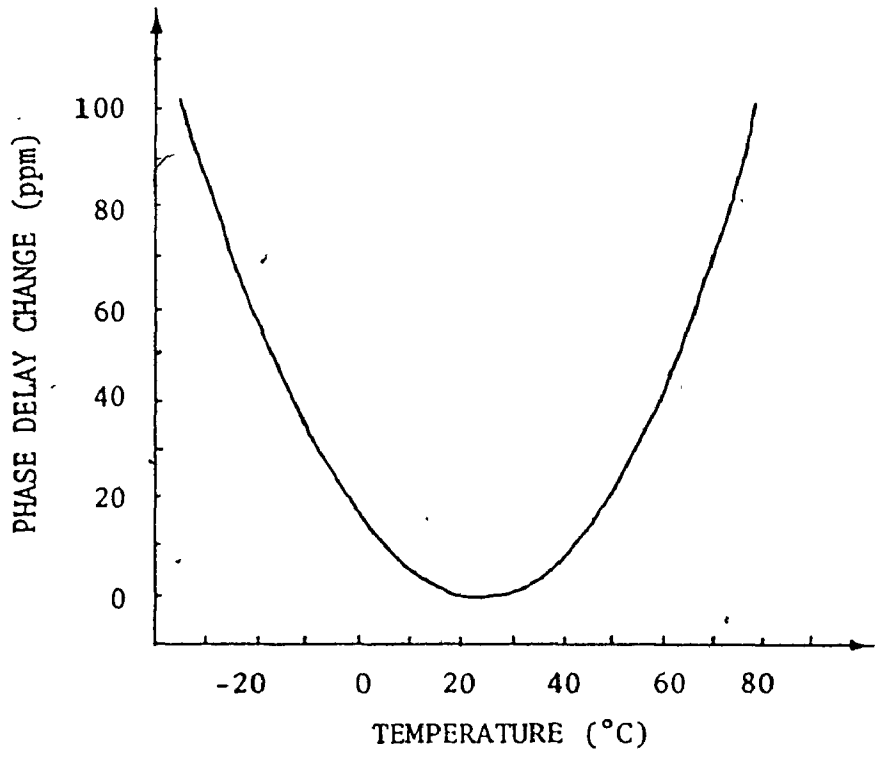

Figure 3.4 Temperature Dependence of ST-X Quartz (θ = 42 3/4°)

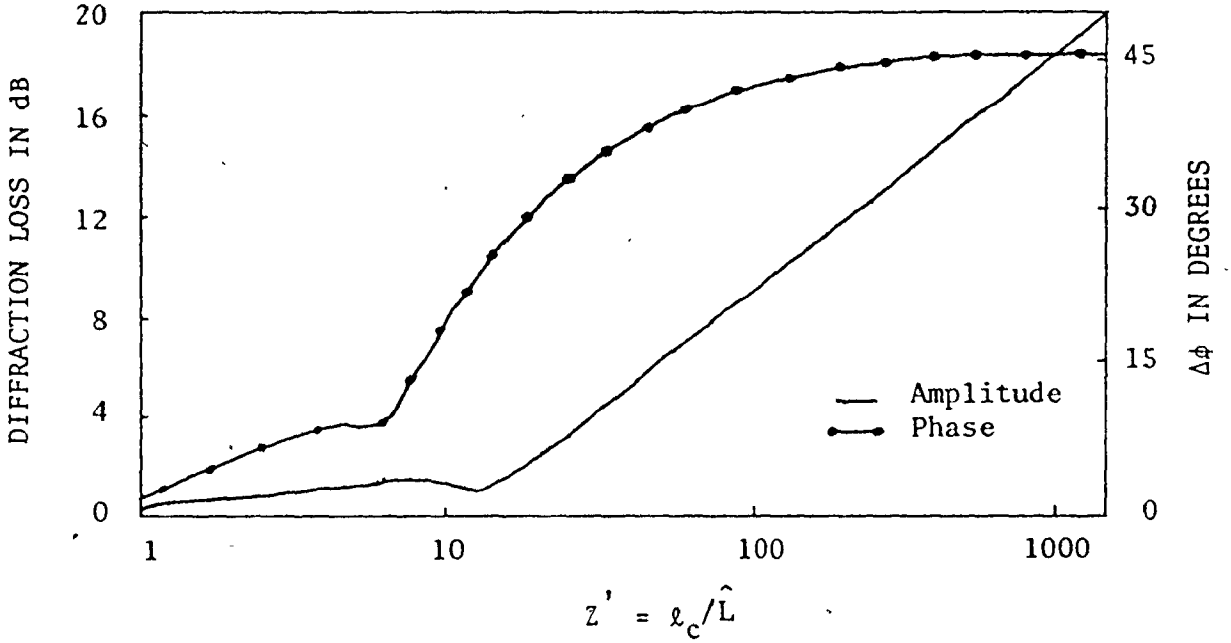

Figure 3.5 Amplitude and Phase Errors Due to SAW Diffraction For ST-X Quartz

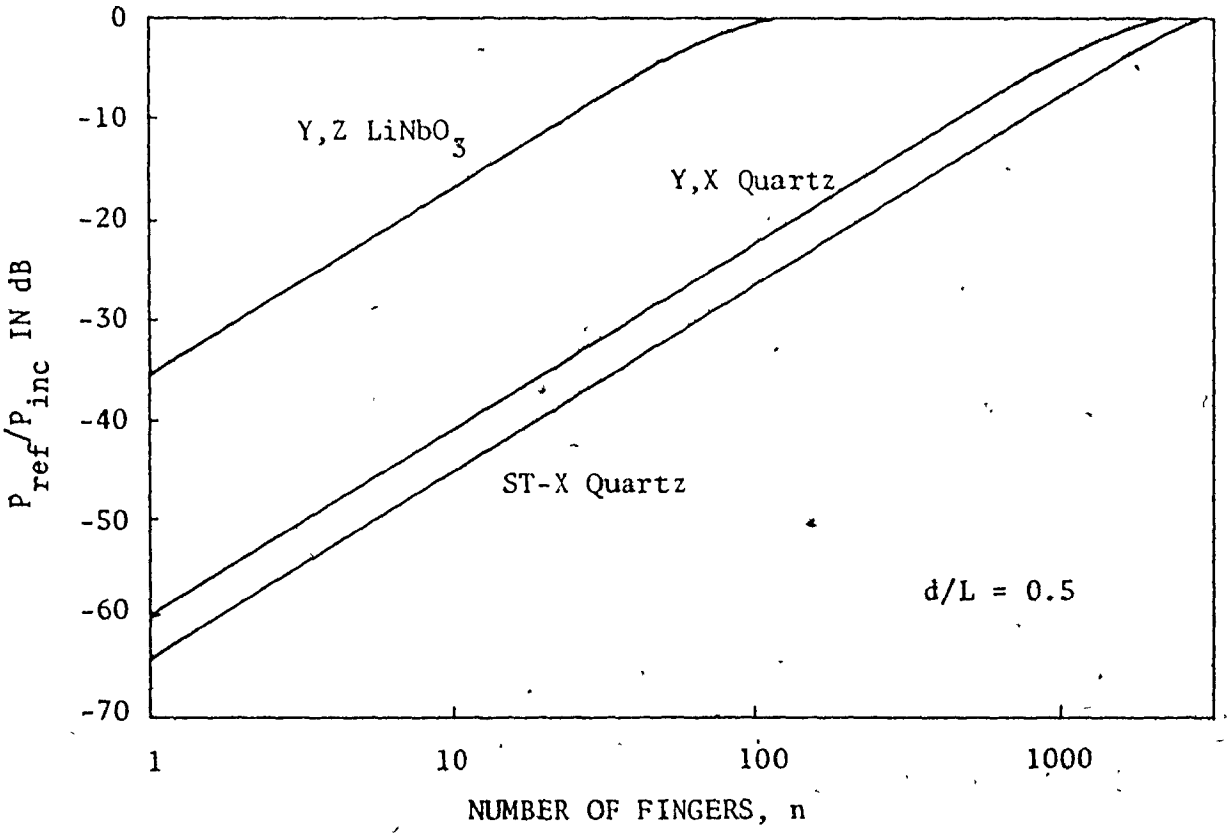

Figure 3.6 SAW Reflections Due to Fingers For Several Common Substrate Materials

for a finger width-to-gap ratio of one.

3.3 Transducer Design

The centre frequency of operation for the SAW oscillator was chosen as 124 MHz since this frequency was within the limits of the available test equipment and production facilities. The resulting acoustic wavelength λ_o is given by:

$$\lambda_o = \frac{v_a}{f_o} = \frac{3158}{124 \times 10^6} = 25.468 \ \mu m \qquad (3.3)$$

The centre design frequency was adjusted to yield a convenient acoustic wavelength for mask cutting purposes, and the final design values were then:

$$f_o = 124.33 \text{ MHz}$$

$$\lambda_o = 25.4 \ \mu m = .001"$$

An aluminum finger thickness of 2000 Å was chosen and therefore no corrections for mass loading effects were made since the finger thickness to acoustic wavelength ratio is very small. The simple two finger-per-wavelength transducer configuration was chosen with a finger-to-gap ratio of one so that the higher harmonics are suppressed. This yields a finger width and spacing equal to $\lambda_o/4 = 6.35 \ \mu m$.

The input transducer length was set to 100 λ_o and the output transducer to 20 λ_o which yields a total delay line length of 160 λ_o. Longer arrays were not possible because of limits in the photolithographic

process available. Hence the input transducer has 201 fingers while the output transducer has 41 fingers. A general program was written on an HP 9100 A calculator-plotter system which plots the theoretical frequency response of a SAW delay line using the results from the Z-transform theory in Chapter II. The finger and frequency values above were entered and the resulting plot is shown in Figure 3.7. From equation (2.18) it is seen that the possible frequencies of oscillation in the loop about the synchronous frequency f_o are:

$$f_{osc.} = f_o + p\frac{f_o}{N} \tag{3.4}$$

where p = integer

N = number of finger pairs

f_o = 124.33 MHz

From Figure 3.7 it is seen that the nodes of the response occur at:

$$f_{node} = f_o + \frac{2mf_o}{n} \tag{3.5}$$

where m = integer, and $m \neq 0$

Since $N = \frac{n}{2}$, the nodal frequencies coincide with all the oscillation frequencies except for f_o which is at a maximum. Hence the mode selection is complete in the design case. Note that the theoretical level of the first sidelobe in the frequency response is -14.4 dB because of the wider

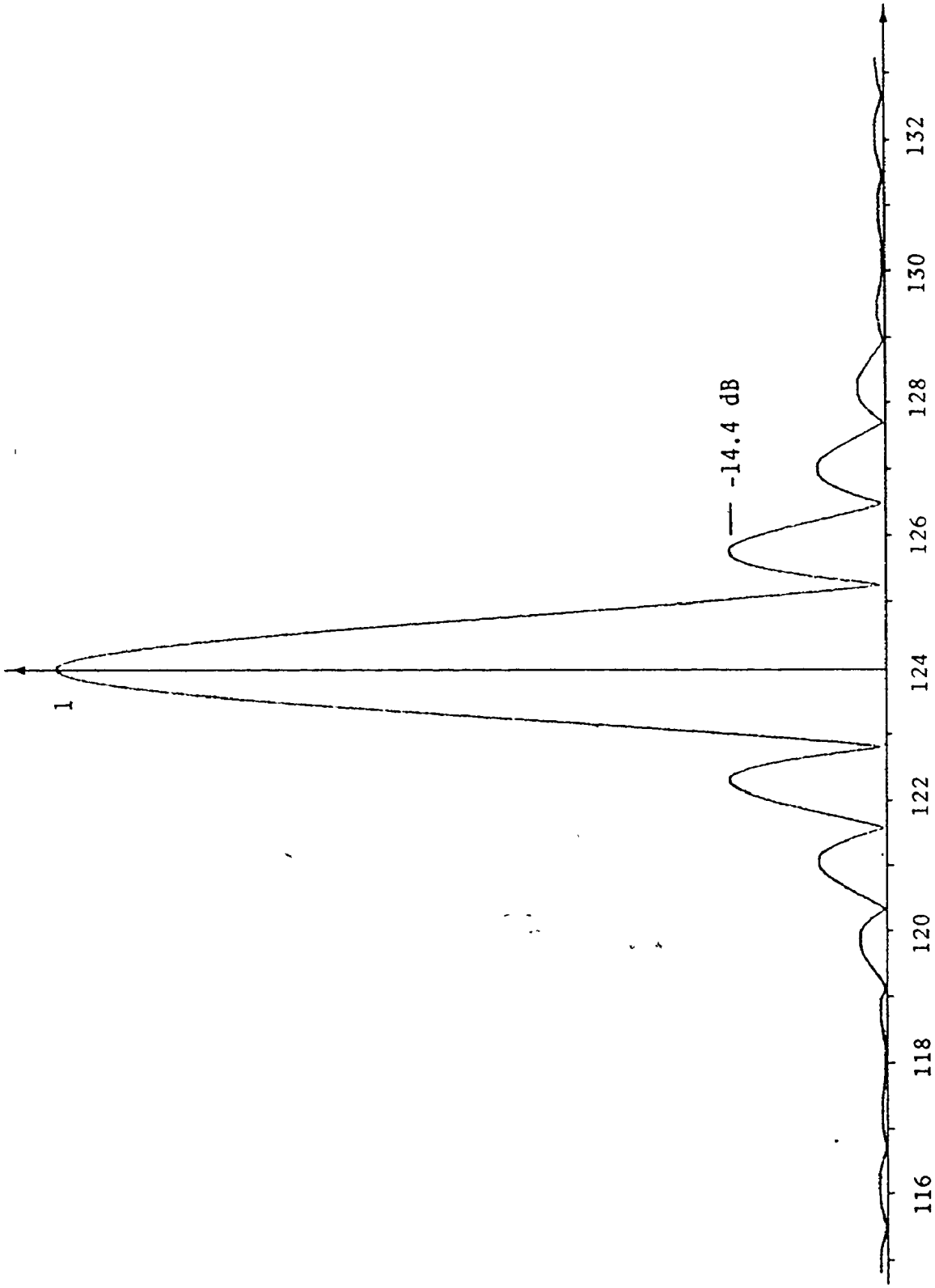

Figure 3.7 Theoretical Frequency Response of Delay Line Design. (Normalized)

bandwidth response of the output transducer. The output transducer was made shorter in length (N = 20) to prevent close proximity to the input transducer and therefore has a wider bandwidth response.

The final design parameter remaining is the acoustic aperture which determines the impedances of the transducers. The reactive impedance of the input transducer should equal 50 Ω at resonance for a minimum untuned insertion loss. [15]. Therefore at f_o = 124.33 MHz:

$$\left| \frac{1}{j\omega_o C_{T_1}} \right| = 50$$

$$C_{T_1} = 25.67 \text{ pF} \tag{3.6}$$

Equations (2.19) to (2.21) can be used to determine the required aperture width $\hat{L}$ as follows:

$$\epsilon_{PR}^{T} \approx 4.6 \quad \text{for quartz}$$

$$C_{FF} \approx 50.8 \text{ pF/m for quartz}$$

$$\hat{L} = \frac{C_{T_1}}{C_{FF} N_1 \lambda_o} = 198.94 \text{ wavelengths} \tag{3.7}$$

where N_1 = 100 finger pairs

$$\lambda_o = 25.4 \times 10^{-6} \text{ m.}$$

For simplicity, the aperture width was set to 200 wavelengths long which yields an output transducer capacitance C_{T_2} of:

$$C_{T_2} = C_{FF} N_2 \hat{L} \lambda_o \approx 5.2 \text{ pF} \tag{3.8}$$

Hence the output transducer reactive impedance becomes:

$$\left| \frac{1}{j\omega_o C_{T_2}} \right| \approx 247\ \Omega \tag{3.9}$$

The effective loaded Q [8] of the SAW oscillator is given by:

$$Q_L = \frac{2\pi \hat{L}}{\lambda_o} \approx 628 \tag{3.10}$$

The completed transducer design is shown in Figure 3.8 along with the sloping connection pads to prevent capacitance effects from parallel edges.

3.4 Delay Line Fabrication Procedure

A mask was generated of the delay line at a 100X enlarged scale. This was done by cutting the pattern in red rubylith (Ulano #Q7261) on a Haag Streit AG 1200 x 1200 mm cutting table. With finger widths of approximately 6 microns it was decided to use chemical etching to produce the final circuit, and therefore a positive mask was cut since two photo-reduction steps were involved. The completed pattern in rubylith measured 21.5" by 25" and was photoreduced by a factor of 5 using a Nuarc STT1418 camera system. (facility of McMaster Audio Visual Centre). The resulting negatives are on 8.5" x 11" Kodak high resolution film and are further reduced by a factor of 20 on the Microkon 1700 camera system onto 2" x 2" x .06" high resolution Kodak plates.

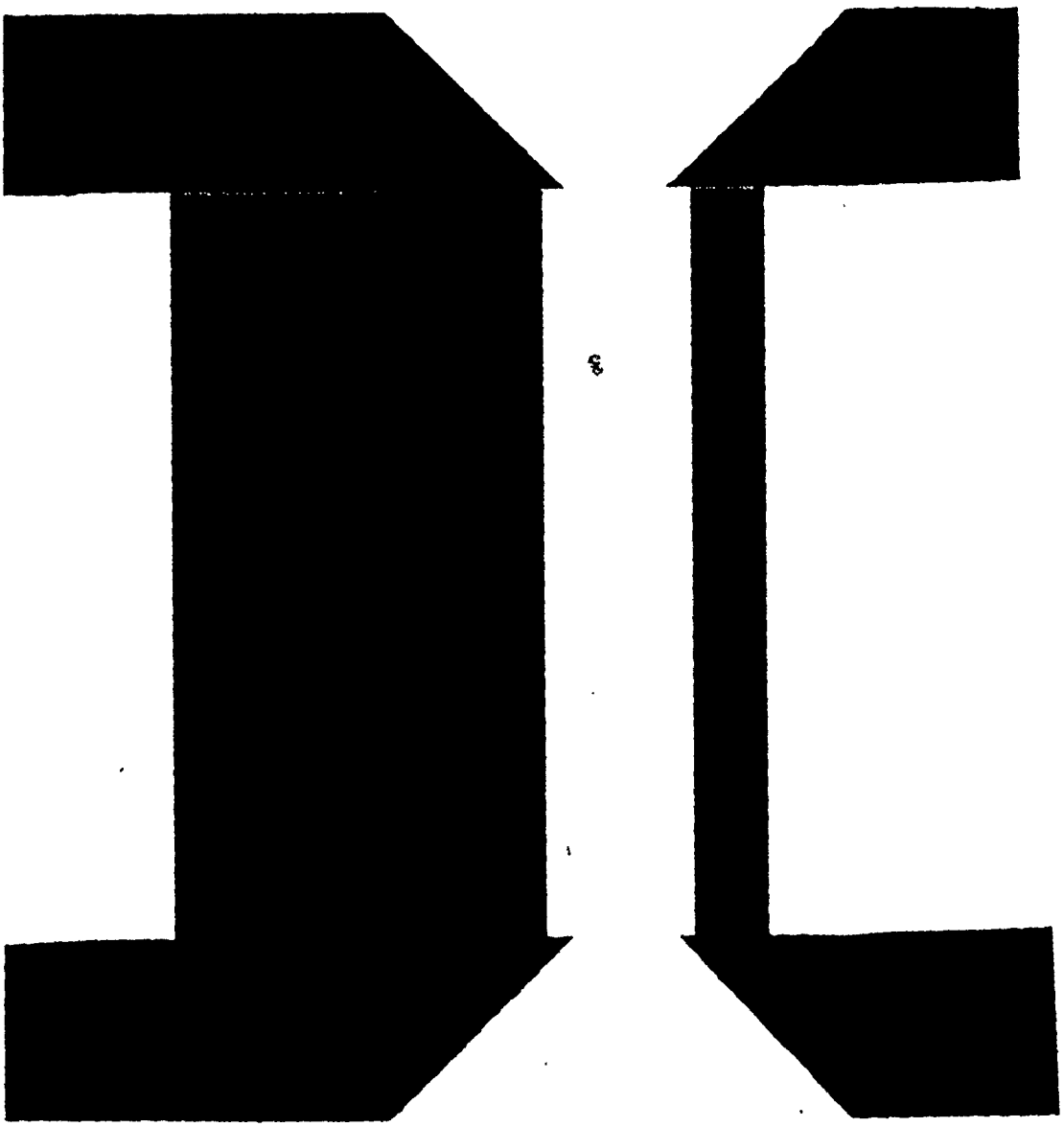

Figure 3.8 Completed Design for 124 MHz SAW Oscillator Delay Line (Enlarged 20X)

Once the positive mask was finished, the following steps were followed to produce the finished delay line on a piezoelectric substrate:

(1) Substrate Cleaning

The ST-X quartz substrate was immersed in a bath of heated trichloroethylene (50°C) and ultrasonically agitated in this bath for 3 minutes. It was found that the best method of handling the substrate was with very thin-nosed metal tweezers at the corners. Immediately upon removal from the ultrasonic cleaner the substrate was rinsed continuously with acetone for 1 minute and then rinsed under running de-ionized water for 3 minutes. The substrate surface was then slowly and carefully blown dry using Freon gas. The entire cleaning procedure should take place on a clean-air bench or in a dust and climate-controlled room to prevent contamination.

(2) Vacuum Deposition of Thin Film

A complete detailed procedure on the vacuum deposition of a thin film is given in [3] with reference to the same equipment used for this work. After blow drying, the substrate was baked for approximately 20 minutes at 80°C to ensure that any embedded water molecules have left the surface. This ensures that the evaporated thin film will have good adhesion properties. The cleaned substrate was then mounted in an Edwards 12E3 High Vacuum Coating Unit. The chamber was pumped down until a pressure of approximately 10^{-5} torr (mm. Hg) was attained. At this point current was slowly applied to the heating filament inside the chamber which caused the 99.99% pure aluminum to melt and evaporate. A shutter was used to prevent initial foreign particles at the evaporation point from contaminating the substrate surface. The evaporation rate was slow and the thickness

of the evaporated thin film was monitored using the mass loading effect on a resonating bulk wave crystal inside the chamber. The resonating crystal frequency was monitored outside the vacuum unit with a frequency counter. The thin film thickness was derived from the frequency reading by:

$$t = \frac{(3.9)(\Delta f)}{\rho} \tag{3.11}$$

where t = thin film thickness in $\mathring{A}$

Δf = change in crystal frequency

ρ = density of evaporated material

= 2.699 for Al

The evaporation process was terminated when the required thickness was reached. (2000 $\mathring{A}$)

(3) Pattern Transfer to Substrate

The aluminum coated substrate was carefully mounted to a spinner on a clean air bench and spun at 3000 rpm. Several cc's of filtered AZ 1350-B Shipley positive photo resist were applied to the spinning substrate with a hypodermic syringe. After 1 minute of spinning from the time of application, the entire substrate surface should have a thin, evenly-distributed coating of photo resist on the surface. The substrate was then baked in an oven for 20 minutes at 80°C. After removal from the oven the substrate was positioned approximately 12" under an ultraviolet light source (650 Watt projection lamp). The delay line mask was then aligned on the surface of the crystal with the aid of a microscope to ensure that the transducer

fingers were perpendicular to the X-axis of the crystal. After alignment the glass plate mask was weighted-down evenly on the edges to ensure intimate contact with the substrate surface. The photo resist was exposed for 5 minutes after which the exposed areas were developed away with Shipley developer for 90 seconds.

(4) Etching of Pattern:

After rinsing the surface from any residual developer with deionized water, the substrate is ready to be etched. Post-baking is necessary first to cure the resist layer so that it can withstand the etching chemicals. The substrate was therefore baked again for 30 minutes at 80°C. The substrate was then immersed in an aluminum etchant consisting of phosphoric, acetic and nitric acids, mixed by volume in the ratio 25:5:1. The etching process was observed under a microscope so that the substrate could quickly be removed upon completion of the etching process. The substrate was then rinsed off with deionized water and carefully blown dry and inspected for flaws.

Two identical delay lines were fabricated in this manner. A special test enclosure was fabricated for one delay line for testing purposes, and is shown in Figure 3.9. The enclosure was machined from aluminum and OSM type 244-3SF stripline launchers were used for the input and output ports. Shielding was the principle purpose of the enclosure and lead lengths were kept to a minimum since the centre conductors of the launchers were directly connected to the transducer pads. The connections were made using GC Silver Conductive Paint which was also used to bond the substrate to the enclosure at the edges. Apiezon type N vacuum grease was used at the substrate edges for acoustic absorption since this could be

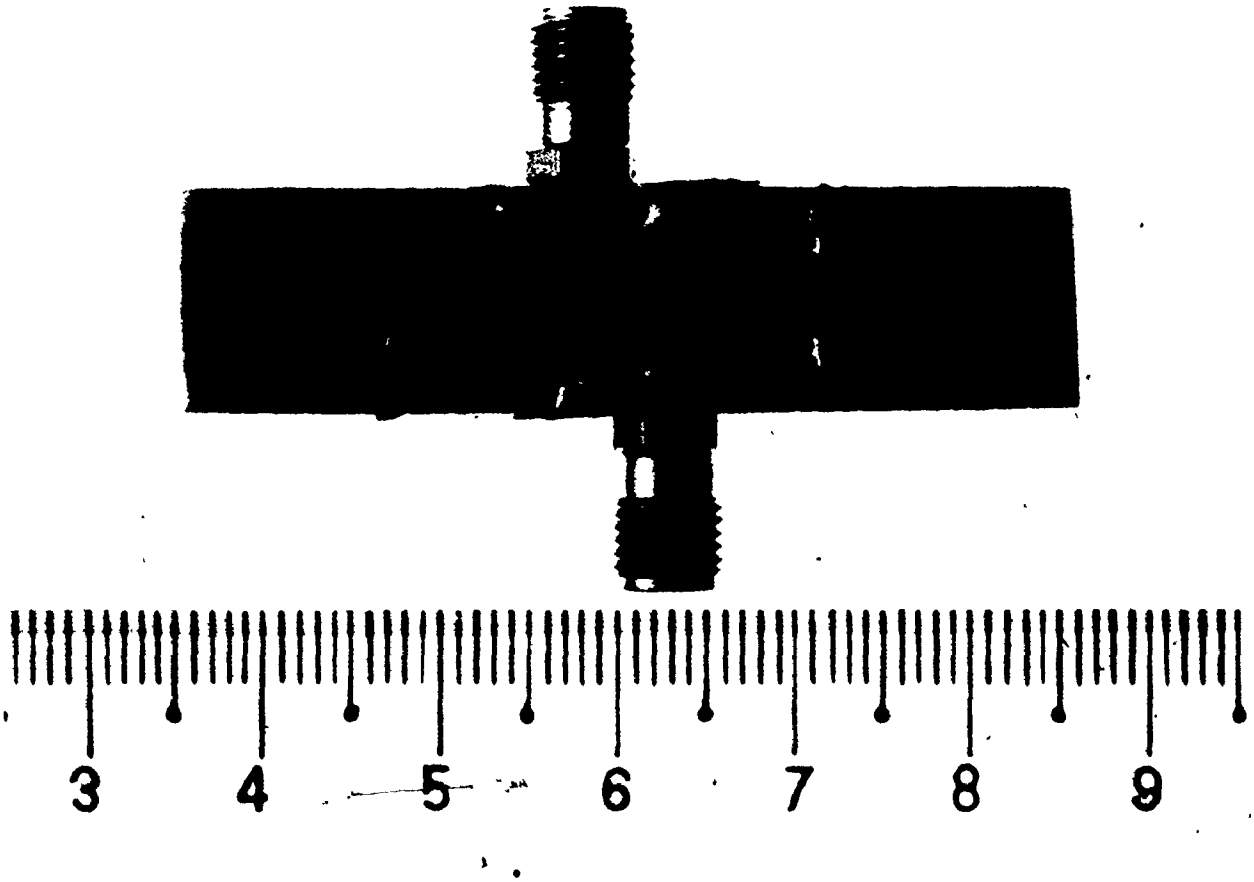

Figure 3.9 Completed SAW Delay Line Mounted in Test Enclosure with Top Removed (Scale in cm.)

easily applied and cleaned as opposed to paraffin. The other delay line was integrated with an amplifier which will be discussed in the following section.

3.5 Integration with Amplifier

The second delay line was incorporated into a microstrip circuit package which included a two stage transistor amplifier. The transistors used in the amplifier were HP 35825-B microwave transistors which were available in a .3" stripline package. (H-Pac 130). The amplifier was designed for a gain of 32 to 34 dB at 124 MHz. It was decided to allow for a variable gain of 2 dB by means of adjusting the dc power supply input voltage for experimental testing purposes.

A fixed bias configuration was chosen for the amplifier stages and the transistor curves were independently measured to aid in the design of the operating point. The input impedance at the resonant frequency was designed approximately to equal the 250 Ω reactive impedance of the output transducer. Similarily, the output stage utilizes 50 Ω microstrip to couple to the feedback loop and the input transducer. The entire circuit except the SAW device itself was fabricated on a 2" x 2" copper-clad dielectric. The design and etching of this board is covered in Appendix I. The coupling capacitors were chosen to provide a low impedance in the order of a few ohms at 124 MHz. Since miniature transformers and inductors were not available, a feedback design of the amplifier was not possible. This resulted in a non-linear frequency characteristic and a decrease in optimum amplifier stability, but these problems were not too serious considering the high Q of the SAW circuit compared to the wider bandwidth of the amplifier.

The physical layout of the circuit is shown schematically in Figure 3.10. The open loop design was incorporated so that experimental testing of the SAW delay line and amplifier charcteristics could take place and also the length of the feedback loop could be adjusted with this design for frequency trimming purposes. The completed device is shown in Figure 3.11. GC Silver Conductive Paint was used to make the connections from the circuit board to the SAW delay line, and Apiezon type N vacuum grease was used at the substrate edges for acoustic absorption.

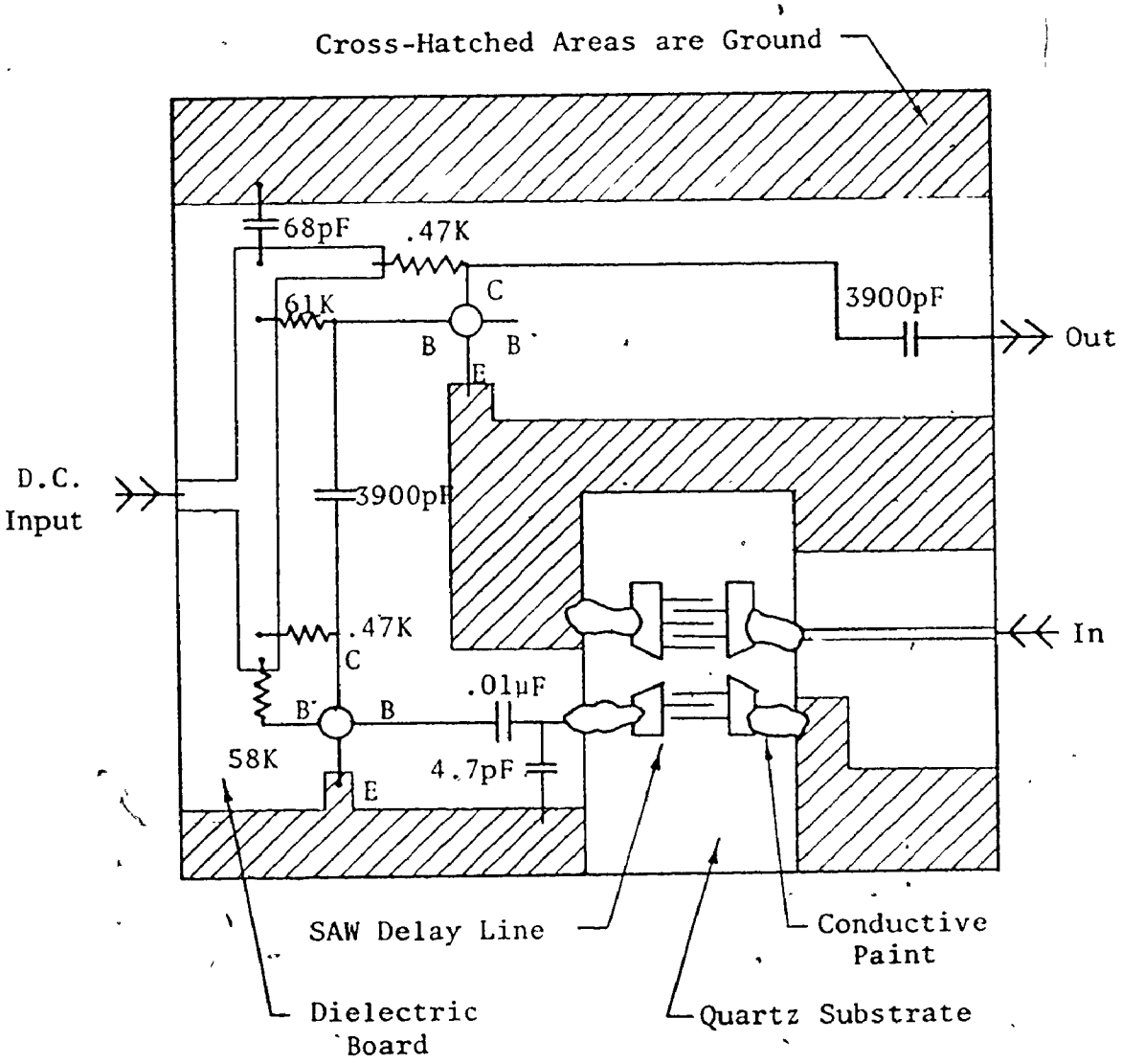

Figure 3.10 Schematic of Physical Layout of SAW Oscillator Circuit

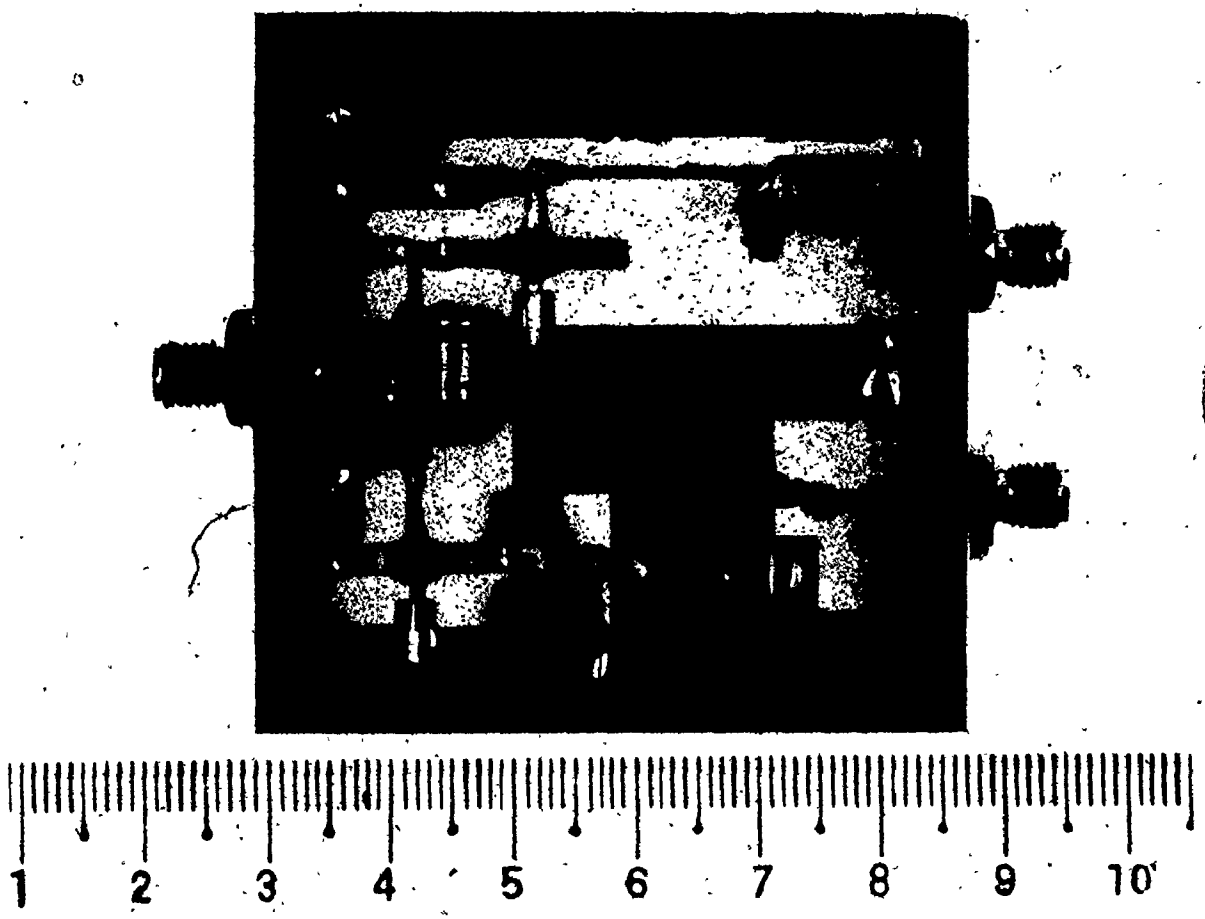

Figure 3.11 Completed SAW Oscillator Circuit
(Scale in cm.)

CHAPTER IV

EXPERIMENTAL RESULTS

4.1 General

Each of the two constructed delay lines was individually tested and compared. The performance of the integrated SAW oscillator was then compared to that of a second oscillator which was constructed with the second SAW delay line using a bank of Anzac AM-102 amplifiers in the feedback loop. For simplicity the integrated SAW oscillator will be referred to as oscillator No. 1 and the second SAW oscillator with the separate delay line and amplifiers will be referred to as oscillator No. 2. Swept frequency measurements were performed on both delay lines. Power output and spectral purity was measured on a spectrum analyzer for both of the oscillators, and short and long-term stability tests were also performed. Impedance measurements were made on the delay lines to determine the accuracy of the design and the design model.

4.2 Delay Line Response

The SAW delay line No. 2 was tested for its frequency response using a Hewlett Packard (HP) 8660B synthesized signal generator in the sweep mode as a source. The output of the delay line was detected and then displayed on a Model 8000 Singer-Alfred oscilloscope using the Alfred Model 7051 sweep network analyzer. All swept-frequency tests were performed using the aforementioned equipment.

The narrow-band response of delay line No. 2 is shown in Figure 4.1. The response peaked at 123.85 MHz which yields an error of less than 0.4% from the design value of 124.33 MHz. This frequency shift is due to a number of factors including mass loading, errors in the photoreduction process for the mask, and variations in the substrate cut angle which produces a slightly different acoustic surface-wave velocity from theory. Insertion loss at the centre frequency was 32.8 dB while the first side-lobe was down 8 dB from the peak. The insertion loss obtained is typical of delay lines on ST-X quartz [17] and is due primarily to mismatch losses and series finger resistance losses at higher frequencies. Upon close examination of the transducers under a microscope it was noticed that approximately 20% of the fingers in both transducers were possible open circuits due to very fine scratches on the surface. This would alter the frequency characteristic of the passband and in particular would account for the 8 DB difference between the side lobes and the peak of the response compared to the theoretical 14.4 dB. It was also noticed that the actual finger width-to-gap ratio was 0.6 instead of 1.0. From [10] this would result in a decreased output at the fundamental frequency and an increase in the 3rd, 5th and 7th harmonic outputs. The reason for the increased gap width is due to the photo-mask used and chemical undercutting. The mask on the 2 x 2 inch glass plate could not make intimate contact with the substrate surface because of the rigidity and awkwardness of its large size compared to the size of the substrate, and also because of the small linewidths ($\sim$ 6 μm) involved. Undercutting from the chemical etching process also accounts for the wider gap widths.

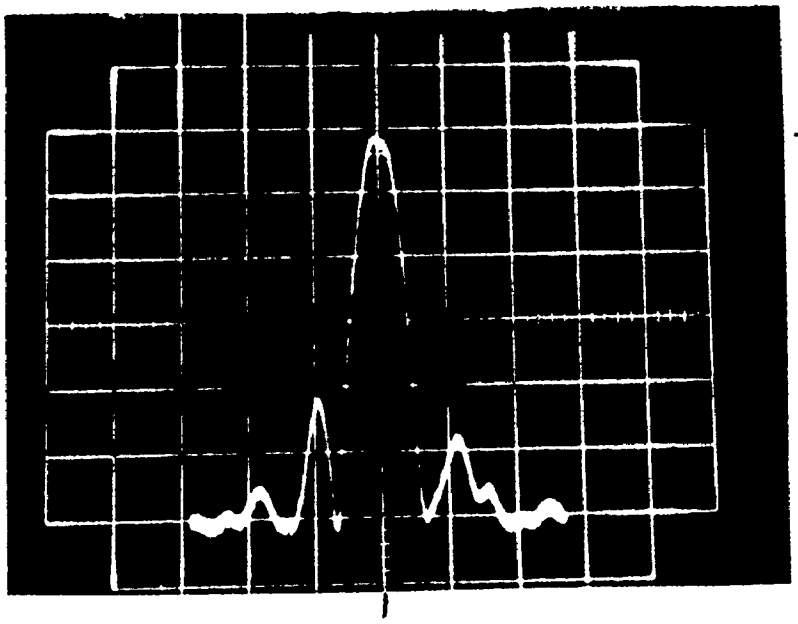

123.85 MHz

Vertical: 2dB/div.

Horizontal: 10 MHz Sweep

Figure 4.1 Frequency Response of SAW Delay Line No. 2

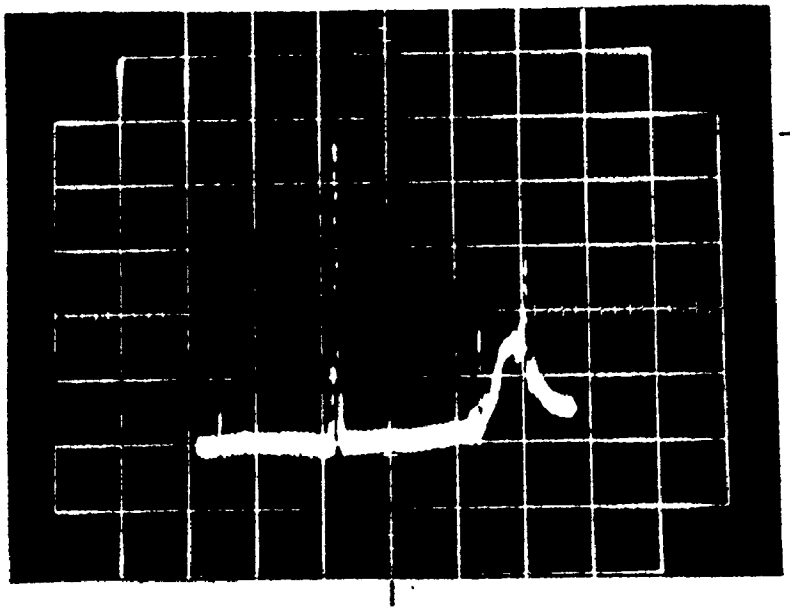

150 MHz

Vertical: 2dB/div.

Horizontal: 200 MHz Sweep

Figure 4.2 Overall Frequency Response of SAW Delay Line No. 2

The dip occuring in the upper side-lobe in Figure 4.1 is due to phase cancellation occuring at that frequency. The first nulls occur at $\approx f_o \pm 1.2$ MHz which agrees with the result in the design case given by equation (3.5).

Figure 4.2 shows the overall frequency response of SAW delay line No. 2. The general rise of the response at approximately $2f_o$ is due to bulk mode coupling between transducers and was demonstrated experimentally by observing the frequency response after a few drops of acetone were placed on the surface of the substrate between transducers to absorb the surface waves. The sharp peak occuring at $2f_o$ is the second harmonic response of the transducers.

SAW delay line No. 2 was then connected to four Anzac amplifiers at the output and similar swept-frequency measurements were made under the condition of 0 dB overall gain in the open loop. The results are shown in Figures 4.3 and 4.4 and no appreciable change in the response is noticed other than a slight sharpening of the response peak at f_o.

Swept-frequency measurements of SAW delay line No. 1 were not made independent of the amplifier since it was immediately incorporated into the overall oscillator circuit. Figure 4.5 shows the in-band response about f_o of the open loop under the condition of 0 dB loop gain. Phase cancellation at approximately f_o is causing the dip in the response curve near the centre frequency. The first nulls about f_o occur at approximately f_o/N from the centre frequency as predicted. The added nulls in the response are due to phase cancellations at the appropriate frequencies which can arise from unwanted reflections or mode coupling. These

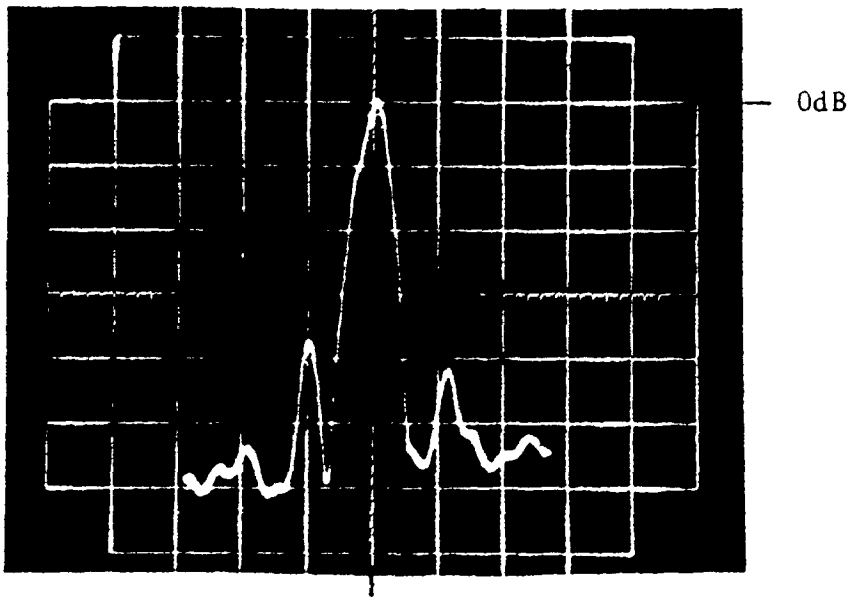

Vertical: 2dB/div.

Horizontal: 10 MHz Sweep

Figure 4.3 Open Loop Frequency Response of SAW Oscillator No. 2 with 0dB Gain

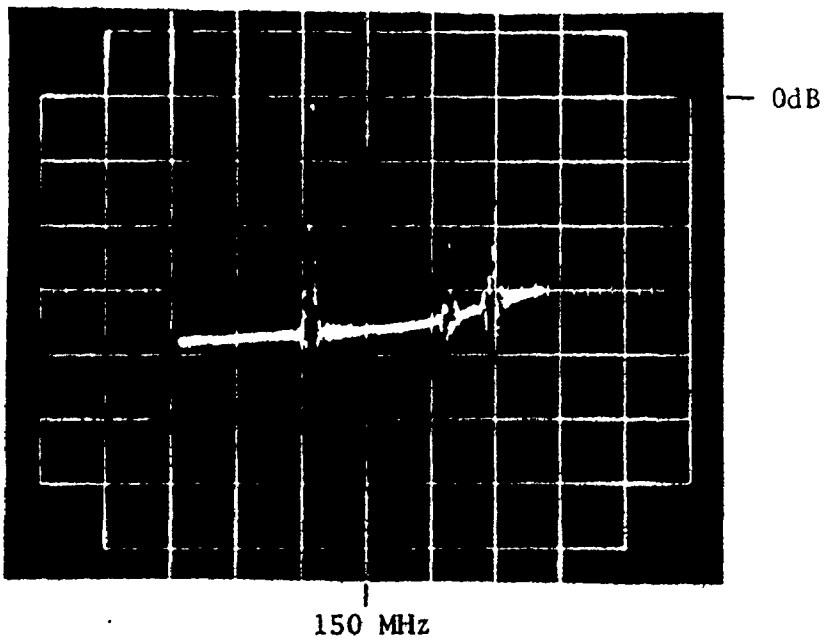

Vertical: 5dB/div.

Horizontal: 200 MHz Sweep

Figure 4.4 Overall Open Loop Frequency Response of SAW Oscillator No. 2 with 0dB Gain

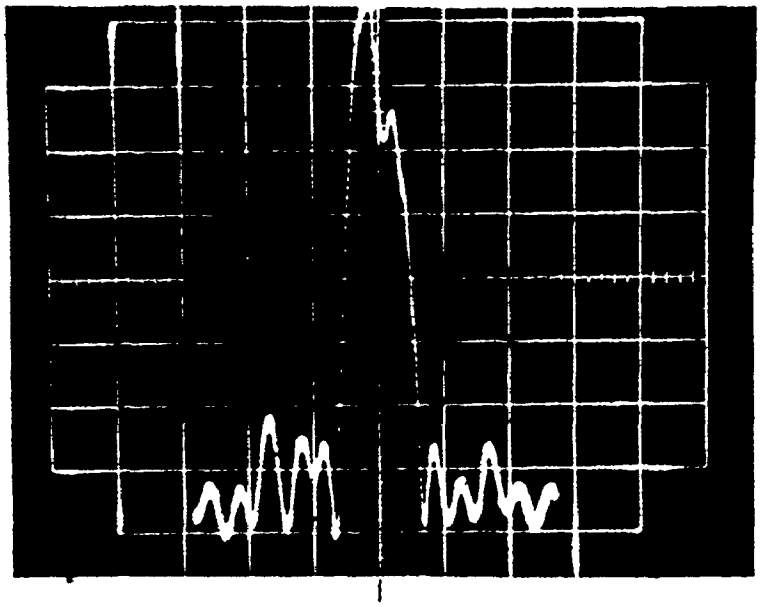

Vertical: 2dB/div.

Horizontal: 10 MHz Sweep

Figure 4.5 Open Loop Frequency Response of SAW Oscillator No. 1 with 0dB Gain

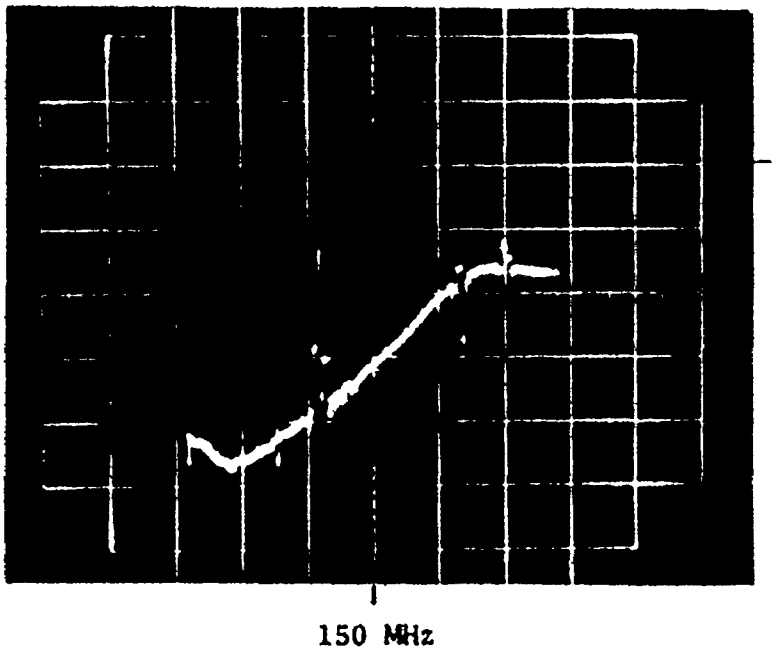

Vertical: 5dB/div.

Horizontal: 200 MHz Sweep

Figure 4.6 Overall Open Loop Frequency Response of SAW Oscillator No. 1 with 0dB Gain

reflections could occur from a group of fingers which are open-circuited or a combination of open and short circuits in the fingers which would cause other frequency modes to be coupled out of phase with the fundamental and thus effect phase cancellation. Some of the nulls may also be caused by the circuit elements in the amplifier; however the exact origins of the nulls were not investigated since their occurrence was advantageous in keeping the level of the first side-lobes down. The first side-lobe level was down 12.5 dB which is a marked improvement over delay line No. 2. The actual centre frequency of this delay line would be 124.7 MHz if it were not for the presence of the dip in the response. With the phase cancellation taking place, the peak of the response occurs at 123.4 MHz which produces a larger error of 0.75 % compared to the theoretical centre frequency of 124.33 MHz.

Figure 4.6 shows the overall open loop response of SAW oscillator No. 1. The rising of the response with frequency is due to feedthru problems associated with the layout of the circuit and amplifier design. The second harmonic is down about 7 dB, which was considered sufficient to prevent mode hopping. The insertion loss at the centre frequency (i.e. the peak at 123.4 MHz) was measured earlier and found to be 31.5 dB.

4.3 Impedance of Transducers

Tests were conducted on SAW delay line No. 2 to determine the input and output impedances. The results obtained using a General Radio 1620-A capacitance bridge at a frequency of 10 KHz were as follows:

Input Transducer: $C_{T1} = 16.2$ pF

$R_{a1} = 3.42\ \Omega$

Output Transducer: $C_{T2} = 1.9$ pF

$R_{a2} = 14.4\ \Omega$

The radiation resistance R_a above is the series radiation resistance and therefore also includes the series resistance of the transducer fingers and any connections to the transducer pads. These values differ appreciably from the theoretical values obtained in Chapter III. One reason for the discrepancy is that the bridge measures the capacitance presented by the coaxial adaptors or connectors used in attaching the SAW device to the bridge. The adaptors could be measured independently and the resulting value subtracted from the value attained with the SAW device connected. The capacitance of the OSM launcher (physically attached to test structure) and any stray capacitances associated with the packaging are unfortunately included in the readings. The second reason for the discrepancy in the readings on the bridge is due to the fact that the permittivity of the substrate is frequency dependent.[27]. .Better results would be obtained if the operational centre frequency of the device were used for the bridge measurement. However, the problem of measuring the connector and stray capacitances along with the actual transducer capacitance still exists.

In view of the above measurement problems it was decided to use a new approach in measuring the transducer impedances. Single-stub matching from transmission line theory was used to match the SAW delay

line to a 50 Ω air-line system. The experimental set-up is shown schematically in Figure 4.7. A directional coupler was used to monitor the reflected wave, instead of using the conventional slotted line and VSWR (voltage standing wave ratio) indicator. A General Radio Type 1021-A UHF standard signal generator was used as the source. The frequency was set to the centre frequency of the SAW delay line and was monitored using an HP-5340A frequency counter. The centre frequency was 35% amplitude-modulated at 1 KHz and amplified with three Anzac AM-102 amplifiers to attain a 0.5 V peak-to-peak voltage into 50 Ω. An HP 8721-A directional bridge was inserted just before the tuning stub and its output was detected and monitored on an FXR Type B812A VSWR indicator. The procedure for attaining a matched load condition is relatively simple. After the SAW device is connected to the end of the transmission air line, the coaxial line-stretcher is varied in such a way as to attain a minimum reading on the VSWR meter. Then the variable short-circuit stub is adjusted to attain a new minimum reading and the process is repeated until an absolute minimum reading is attained. This condition indicates that a minimum amount of reflected power is present and therefore all or most of the incident power is dissipated in the load (SAW transducer) yielding a matched condition. The length of the short circuit stub and the length from the stub to the load can then be used to calculate the complex impedance of the load at the centre frequency of operation with reference to a 50 Ω system. The theory of single-stub matching is covered in [28] and the technique and mathematical relationships used to obtain the impedance of the SAW transducer from the given lengths is covered in

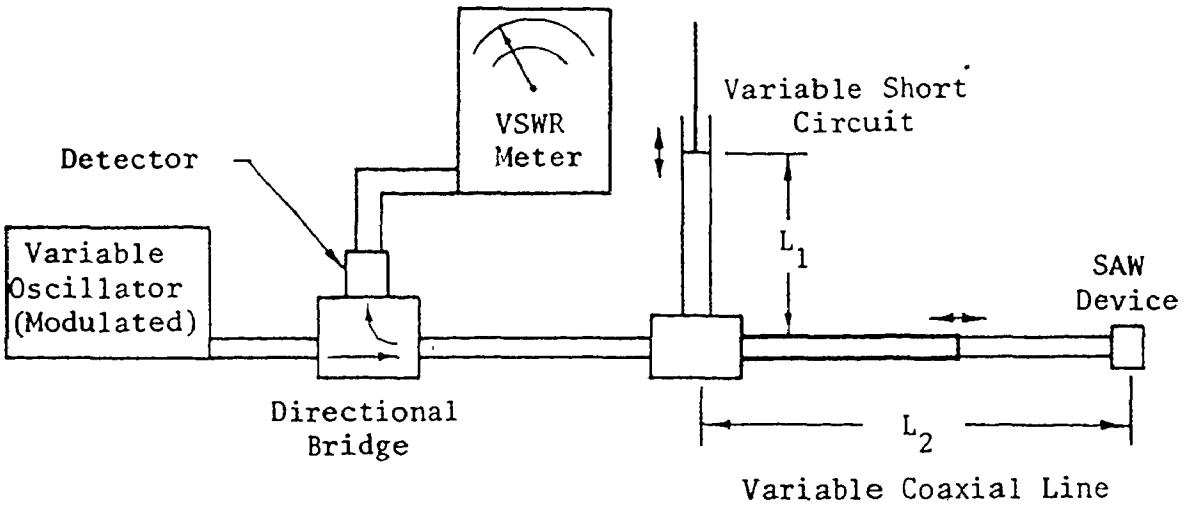

Figure 4.7 Experimental Set-Up for Measurement of SAW Transducer Impedance using Single-Stub Matching

	Radiation Resistance R_a		Total Capacitance C_T		Impedance $\|Z_o\|$	
	Theory	Expt.	Theory	Expt.	Theory	Expt.
Input Transducer	10.14Ω	14.21Ω	25.81pF	26.92pF	50.8Ω	49.8Ω
Output Transducer	10.14Ω	17.33Ω	5.2pF	6.95pF	247.3Ω	185.7Ω

Figure 4.8 Comparison of Impedance Measurements Made on SAW Delay Line No. 2 with Theory

Appendix II. A computer program was written on an HP 9100A programable calculator which calculated the equivalent series radiation resistance and total capacitance of a SAW transducer, given the two tuning lengths and the centre frequency of operation. The results of tests made on SAW delay line No. 2 are shown in Figure 4.8. These results show a much better agreement to the theoretical values keeping in mind that the theoretical radiation resistance does not take into account the finger and connection losses.

The method of single-stub tuning has several advantages. It is a simple and fast method of measuring the complex impedance of a SAW device and is effective from 100 MHz (limited by long wavelengths) up to several gigahertz. The two tuning lengths obtained from the single-stub matching technique can also be used to permanently match the SAW device to a 50 Ω system. This concept will be discussed further in Chapter V.

SAW delay line No. 2 was also tested on an HP 8545-A automatic network analyzer. Initial tests performed on the input transducer yielded an input VSWR of 7.13 and an insertion loss of 38.3 dB at the centre frequency. These results were found to be erroneous and were later credited to the instability of the internal oscillators of the network analyzer. It was therefore concluded that the network analyzer was inappropriate for automatic measurements on extremely narrowband (< 2MHz) devices. However, the network analyzer was used in the manual mode for simple qualitative tests and was found to be quite practical because of its S-parameter switching and test facility. The network analyzer and

other test equipment used to obtain the test results for this thesis are shown collectively in Figure 4.9. The HP 8545-A automatic network analyzer and its associated peripherals are shown in the centre and to the left of Figure 4.9. The HP 8660B frequency synthesizer is shown in the right-centre with the HP 5340A frequency counter on top. An HP-Harrison 6206B dc power supply situated above the frequency counter is used as the power source for the SAW oscillator. The Singer-Alfred Model 8000 oscilloscope along with the Model 7051 sweep network analyzer is situated at the bottom far-right of Figure 4.9, displaying the frequency response of the SAW delay line. Finally, the HP 8555-A spectrum analyzer (RF Section) along with the HP 8552-B I.F. section is shown on top of the Singer oscilloscope.

4.4 Frequency Stability and Trimming

All frequency stability tests were performed only on SAW oscillator No. 1. Only the short and medium-term stabilities were studied since the time involved for long-term aging effects is too lengthy. The open loop of SAW oscillator No. 1 was completed by means of a Merrimac PDM-20-110 power splitter. One output of the power splitter was used to complete the feedback loop by means of a short piece of RG-174/U coaxial cable while the other output served as a test point and oscillator output port. A dc input voltage of ≈ 12 volts was used for the SAW oscillator during the frequency stability tests which were conducted under the conditions of normal output power and best spectral purity. (to be determined in the next part of this Chapter). In order to obtain accurate frequency

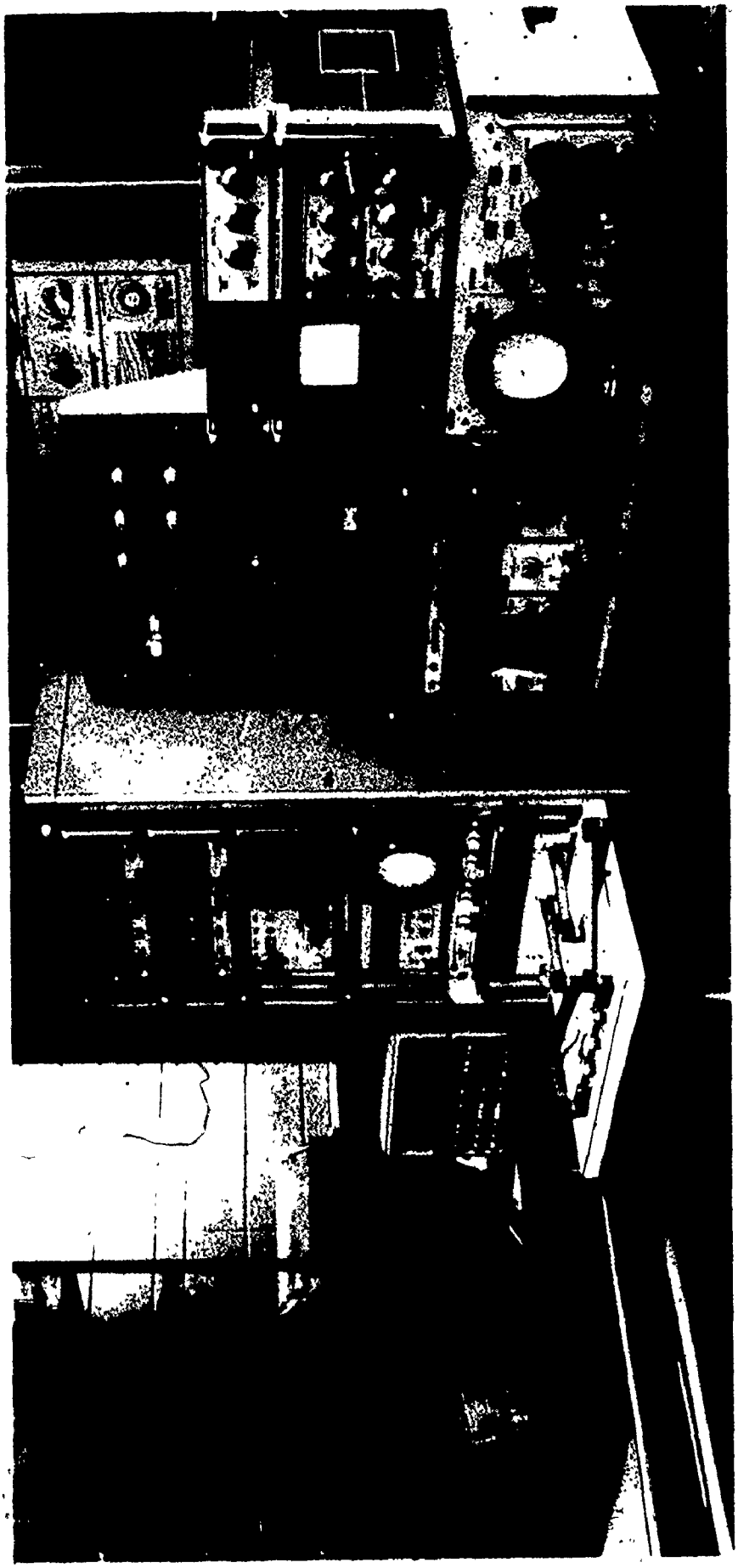

Figure 4.9 Test Equipment Used to Test the SAW Devices

readings with fast gate times on the frequency counter it was decided to mix the SAW oscillator output with a frequency standard of 120 MHz and monitor the difference frequency. The HP frequency synthesizer was used as the frequency standard and an Aertech-Orthostar MX4001 mixer/modulator was used to mix-down the SAW oscillator output with the frequency standard. The mixer output was then amplified using an HP 8447F combination pre-amp/amplifier and monitored with an HP 5216-A 12.5 MHz electronic counter which also served as the low-pass filter for the mixer output. A thermometer was positioned directly beside the oscillator package to monitor the air temperature. Temperature and frequency readings were then taken approximately every 15 minutes for 12 hours.

The result of the medium-term stability test is shown in Figure 4.10. The total stability over a twelve hour period is in the order of 7.5 ppm. Allowing for a complete cyclic change in frequency the resulting frequency deviation would be slightly less than 5 ppm per °C. The short-term stability was determined over a period of 1 second and resulted in a short-term frequency stability of better than 2 parts in 10^7. Stability figures for similar oscillators (tested at constant temperature) [6] yield short-term stabilities of approximately one part in 10^9 and a medium-term stability of less than 1 ppm. The primary reason for the large frequency deviation obtained with SAW oscillator No. 1 is the termperature instability of the amplifier. The author in [8] has shown that some amplifiers can change the zero slope temperature T_o of the characteristic curve for the substrate by as much as 40°C, depending on the quality and design of the amplifier. If T_o is taken as $\sim$ 20°C for

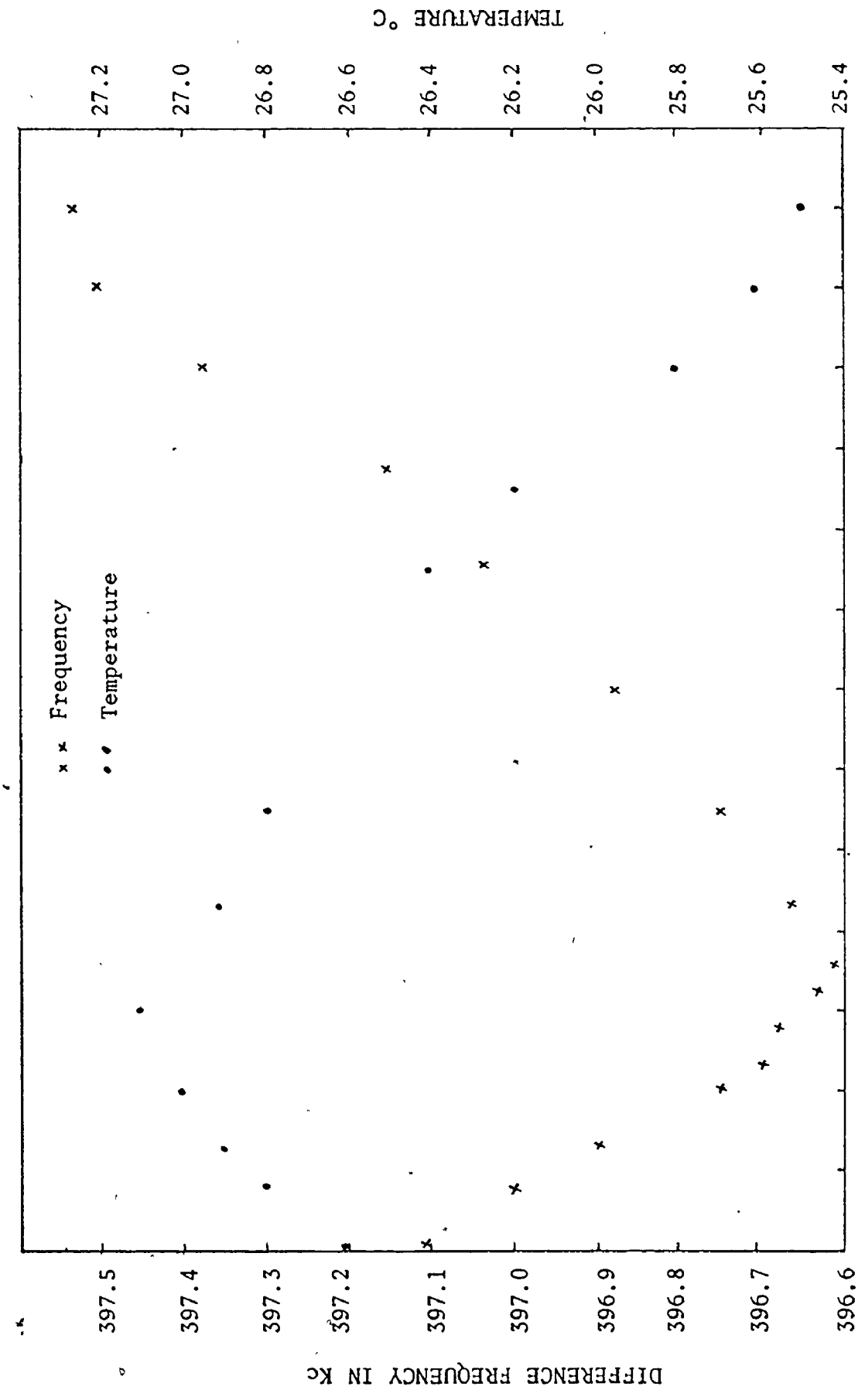

Figure 4.10 Spectral Response of SAW Oscillator No. 1

ST-X quartz, then taking the worst-case condition of a very temperature-sensitive amplifier, T_o will be shifted to -20°C. The author in [9] has shown that the percentage of the acoustic path which is metallized also has an effect of shifting T_o. The metallization ratio for the SAW oscillator tested was $\sim$ 35% and from the results in [9] this yields an additional downward shift of T_o by $\sim$ 12°C. Substituting the resulting zero-slope temperature of T_o = -32°C into equation (2.24) yields a theoretical frequency deviation of $\sim$ 6 ppm for the temperature range encountered in the experiment. This is in fairly close agreement with the experimental result considering that the substrate heat-sinking and overall packaging of the device are not accounted for in the theoretical calculation. If the oscillator under test were forced to put out more power, the phase variations in the amplifier would become even larger and medium-term frequency stabilities in the order of 100 ppm could result for SAW pathlengths of 100λ. [29] Maximum phase deviations in amplifiers occur when they are near or at the saturation level which is why high power, low noise amplifiers are recommended for SAW oscillator synthesis.

Frequency trimming is a necessary condition for any oscillator since there will always be certain error factors in the design or construction process. It is difficult with SAW oscillators to characterize the combined effects of mass loading, temperature drift and phase changes in the amplifier with any accuracy. Hence a frequency trimming process must be readily available and this condition can be satisfied by the insertion of a phase-shifting network in the oscillator feedback loop. Adding a variable phase shift of $\pm \pi/2$ to the loop and neglecting the

(theoretically) constant phase shift due to the amplifier produces a total frequency deviation of : (from equation (2.13))

$$\frac{2\pi f_A \ell}{v_a} \pm \frac{\pi}{2} = 2p\pi \qquad (4.1)$$

$$\frac{\Delta f_A}{f_A} = \mp \frac{\lambda}{4\ell} \qquad (4.2)$$

where f_A = centre frequency (allowed) of oscillator

λ = acoustic wavelength

ℓ = acoustic pathlength between transducers

With a pathlength of $\ell = 100\lambda$ the total frequency deviation becomes $\mp$ 2500 ppm. For SAW oscillator No. 1 this would result in a total allowable frequency deviation of approximately $\mp$ 0.31 MHz. With 18 cm of RG-174/U coaxial cable completing the loop of the SAW oscillator, the frequency of oscillation was experimentally recorded as 123.450 MHz. When an extra 18 cm of coaxial cable was inserted in the loop, the frequency of oscillation changed to 123.251 MHz which results in a change of frequency $\Delta f \simeq -0.2$ MHz. Since the electrical length of the RG-174/U coaxial cable is approximately twice its physical length, the frequency change agrees with the theory. In [8] it is suggested that the $\pm \pi/2$ phase-shifting network be an electronic one, inserted immediately after the feedback amplifier. Possible alternatives to this system will be discussed in the next Chapter.

One other method of frequency trimming for small frequency variations consists of inserting a variable capacitor across the output transducer of the SAW delay line. A 5.5 - 18 pF variable air capacitor was connected across the output transducer of SAW oscillator No. 1 and a frequency variation of ± 280 ppm was attained. This application is very useful for making small corrections due to aging, design and fabrication errors, and general changes in temperature.

4.5 Power and Spectral Purity

The power output and spectral purity of SAW oscillator No. 1 was determined from an HP 8555A spectrum analyzer (RF section) along with the HP 8552B IF section. The output from the oscillator was taken from the power splitter and connected directly into the 50 Ω input of the spectrum analyzer. Results are shown in Figure 4.11 where the left edge of the graticule corresponds to 0 MHz with a horizontal scale of 50 MHz/div. The spectral response is displayed in this fashion with the fundamental frequency shifted to the left of the centre line because the lower frequency limit of the spectrum analyzer is only 100 MHz. The second harmonic is -22 dB from the fundamental which displays a power output level of -10 dBm. The 3rd harmonic is down 33 dB from the fundamental and no other appreciable levels of harmonics were visible. Figure 4.12 shows the spectral response of SAW oscillator No. 2 which has very similar characteristics except for a marked decrease in the third harmonic. The third harmonic is down 37 dB from the fundamental and is due to the slightly narrower bandwidth response of the Anzac amplifiers compared to the amplifier in SAW oscillator No. 1.

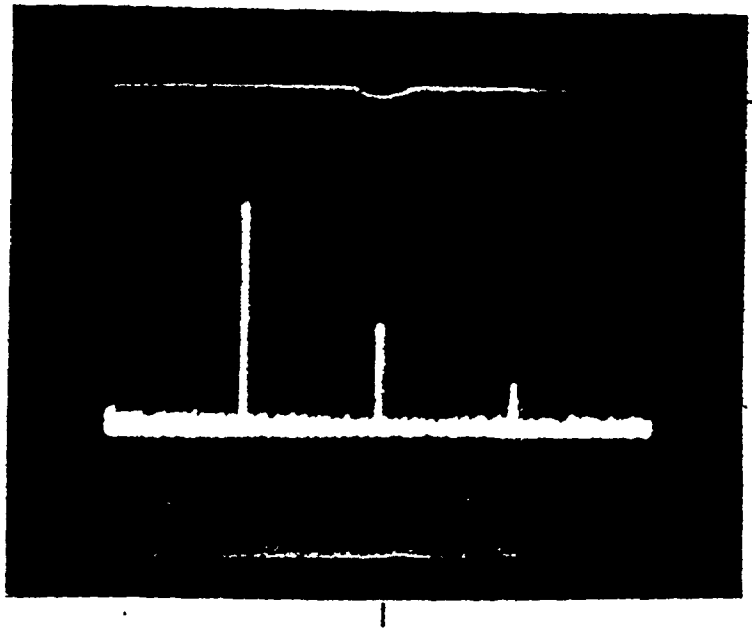

Vertical: 10dB/div.

Horizontal: 50 MHz/div.

Figure 4.11 Spectral Response of SAW Oscillator No. 1

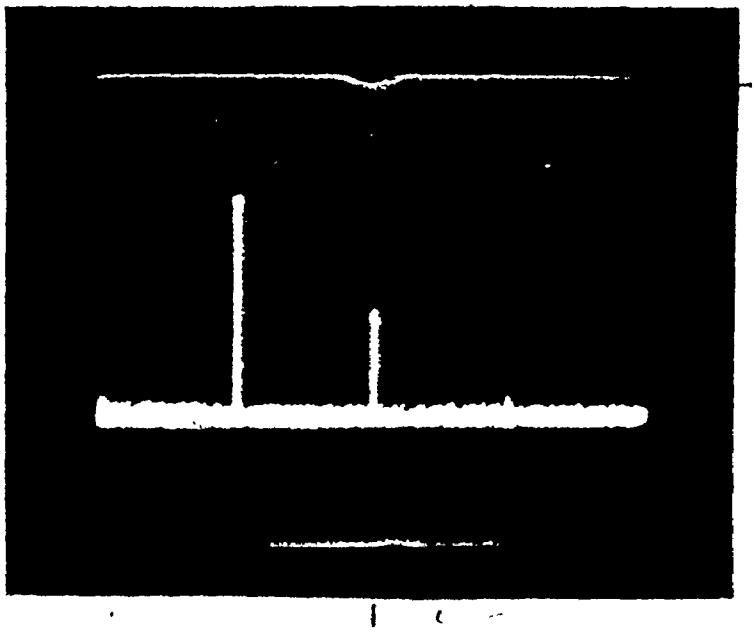

Vertical: 10dB/div.

Horizontal: 50 MHz/div.

Figure 4.12 Spectral Response of SAW Oscillator No. 2

The input voltage to SAW oscillator No. 1 was increased such that the oscillator output was raised to 1 mW. As a result, the levels of the harmonics increased considerably. The second harmonic was down 19 dB, the third 36 dB, and the fourth 54 dB. The harmonic content was increased since the amplifier was supplying more gain and had reached the saturation level.

CHAPTER V

GENERAL CONCLUSIONS

5.1 General

A surface acoustic wave delay line oscillator has successfully been built to operate within 0.4% of the design frequency. The power output and spectral response are moderate while the frequency stability characteristics are relatively good for an oscillator of this type without the use of thermal compensation techniques. The problem of designing the oscillator so that the actual frequency of operation equals the design frequency is not a serious one. The frequency trimming capability of SAW oscillators is ample enough to allow for any effects such as mass loading and errors in the photographic mask. A variation in surface wave velocity for ST-X quartz of 0.25% has been found by the author in the literature [2], [21] and care must be taken to choose the proper value, preferably derived from experimental results since this directly affects the frequency of operation. The frequency stability can be much improved if the entire oscillator is temperature-controlled in an oven. However, this is not always a preferable option when space limitations and maximum efficiency of energy are the primary concerns. Better amplifier designs with regard to temperature insensitivity would also greatly improve the frequency stability of the SAW oscillator. One solution is the use of high power, low noise amplifiers so that the temperature of the amplifier remains moderate for relatively high power outputs. The packaging of the devices in this thesis was designed for

experimental testing purposes and better packaging techniques for permanent operation would contribute to improved operating characteristics. A good solid contact between the substrate and the package would improve the oscillator's thermal stability and its overall ruggedness. The harmonic content in the spectral response of the SAW oscillator is due mainly to the coupling between alternate pairs of fingers which accounts for the 2nd and 4th harmonics, and also due to the finger width-to-gap ratio (spatial harmonics) which accounts for the 3rd, 5th and 7th harmonics. Ensuring that the finger width-to-gap ratio is 1.0 as designed (by allowing for chemical undercutting and photo-mask errors) would alleviate the problem of excessive harmonic content. Alternatively a narrower-bandpass amplifier could be utilized to minimize the harmonic content as long as the frequency characteristic of the SAW delay line remains the frequency-determining element of the oscillator.

5.2 Further Considerations

The technique of using single-stub matching for determining SAW transducer impedances also has a second advantage. The tuning lengths obtained in the measurement process can immediately be used in the process of matching the transducer being measured to a 50 Ω system. It is suggested that stripline techniques be used in implementing the single-stub matching network. At low megahertz frequencies (down to 100 MHz) the electrical tuning lengths can sometimes be quite long (since the electrical wavelength λ is long) depending on the value of the complex load impedance. With the use of high-dielectric copper-clad boards,

($\varepsilon_r > 10$) these long lengths can be reduced to a few centimeters since the phase velocity is decreased relative to the free space value. Hence a SAW transducer can be theoretically perfectly matched at its centre frequency using the single-stub matching technique in conjunction with stripline technology. This method will work equally-well for all frequencies from 100 MHz up to several gigahertz. At higher frequencies, where the tuning lengths become shorter, a lower-value dielectric board can be appropriately chosen so that the required tuning dimensions can be easily realized in the fabrication process. The advantages of this type of matching technique are summarized as follows:

(i) it is a simple transmission line technique

(ii) readily adaptable to any system impedance other than 50 Ω (e.g. matching into a 200 Ω input impedance of an amplifier)

(iii) very insensitive to temperature variations as opposed to L's and C's.

(iv) a planar technique compatible with SAW's

(v) a wide frequency range of application

(vi) the tuning lengths are experimentally pre-determined with a simple experimental set-up rather than relying on theoretical predictions.

(vii) very little energy loss in the matching device itself

One disadvantage of this method is that the match is designed primarily for one frequency and is therefore applicable only to SAW oscillators or narrowband SAW bandpass filters. The bandwidth of this

matching technique in conjunction with a SAW device is a phenomena which has yet to be investigated.

The use of stripline techniques in matching a SAW device implies that the entire feedback loop of a SAW oscillator can be connected with stripline transmission lines. This could be used to advantage in tuning the frequency of the SAW oscillator. The entire $\pm \pi/2$ phase shift can now be realized in a few centimeters of stripline as opposed to an electronic phase shift control at the output of the feedback amplifier. The approximate equivalent electrical length of the stripline circuit can be calculated and used to determine the total loop phase shift (including the known SAW delay line phase shift) and hence the exact operating frequency of the oscillator. A small variable air capacitor can then be used across the output transducer to compensate for any small deviations from the desired frequency due to fabrication tolerances.

Another possible area of investigation is in the use of reflective arrays to modify the $\left(\frac{\sin x}{x}\right)^2$ frequency response of a SAW delay line. The Q of the SAW delay line is dependent on the transducer length. For high Q responses, very long transducers are required which impose greater fabrication problems and have a higher cost since a greater substrate area is used. Reflective arrays could theoretically be used to produce very high Q outputs from moderate-length ($L = 100\lambda$) delay lines by reflecting acoustic energy away from the output transducer at the appropriate frequencies. Figure 5.1 (a) shows the normal $\left(\frac{\sin x}{x}\right)^2$ response of a uniform SAW transducer with the two frequencies f_1 and f_2 which will be affected by the reflective arrays. Figure 5.1 (b) shows the relative position of the two arrays with respect to the SAW delay line. The arrays are positioned close

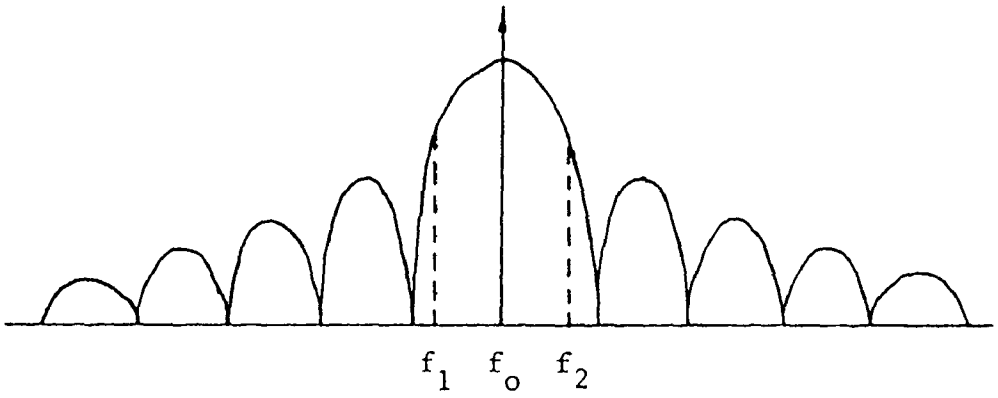

Figure 5.1 (a) Normal $(\frac{\sin x}{x})^2$ Response of SAW Delay Line

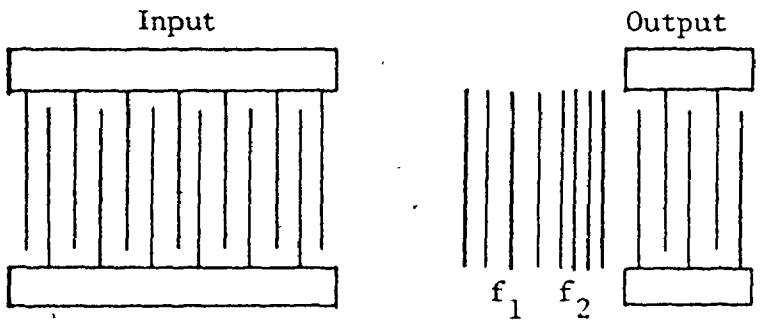

Figure 5.1 (b) Positioning of Reflective Arrays Relative to Delay Line Transducers

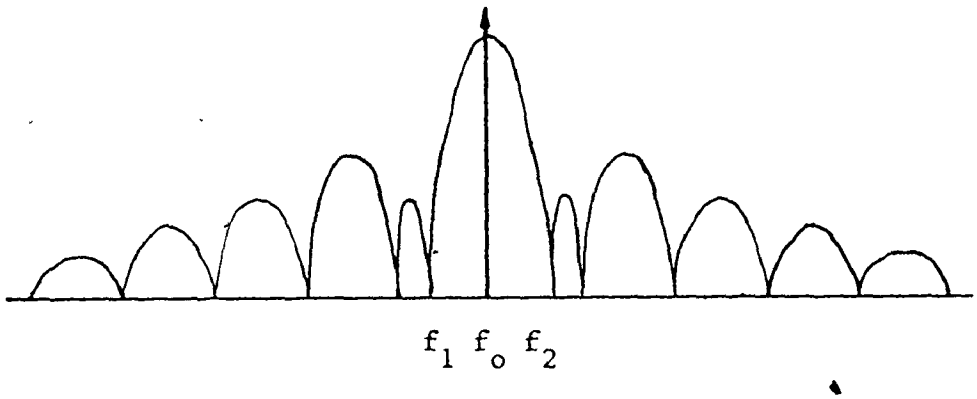

Figure 5.1 (c) Resulting Frequency Response with Reflective Arrays Added

to the output transducer so that the reflected energy will be sufficiently attenuated due to propagation losses before interfering with the input transducer. The resulting (speculated) frequency response is shown in Figure 5.1 (c) where it is demonstrated how the notches produced by the reflective arrays create a higher Q response. The added mass-loading effect due to the reflective arrays is minor, if not negligible and the frequencies f_1 and f_2 can be chosen in such a way as to yield a maximum Q without loss of output at f_o. Further work in this area is needed to determine if the output response can be satisfactorily modified using the reflective array approach.

APPENDIX I

DESIGN AND FABRICATION OF MICROSTRIP TRANSMISSION LINES

The narrow strip approximation (W/H < 1.0) from the work of Wheeler [30] was used in determining the microstrip dimensions. Figure A.1 shows the chart used to determine the ratio W/H, where W is the microstrip width and H is the thickness of the dielectric board. The type of board used was a Custom Materials Inc. High K707L-15 which had a thickness H = .03125" and a dielectric constant of 15. For a 50 Ω transmission line, W/H ≈ .65 from the chart in Figure A.1. This yields a theoretical microstrip width of approximately .02 inches. Figure A.2 shows the completed mask for the 2 x 2 inch circuit cut on red rubylith #9711 on clear 5DR plastic. The 1:1 mask was cut on a Haag-Streit AG Coordinatograph 1200 x 1200 mm cutting table. The following steps were taken to produce the final circuit board:

(1) The copper-clad dielectric board was cut to the appropriate size and then scrubbed with tripoli powder to remove any grease and dirt deposits.

(2) The board was then dipped in a mild ferric cholride solution for 10-15 seconds and then rinsed with HCL solution, followed by a deionized water rinsing for 2-3 minutes. This was the final cleaning step to ensure a dirt and oxidized-free surface.

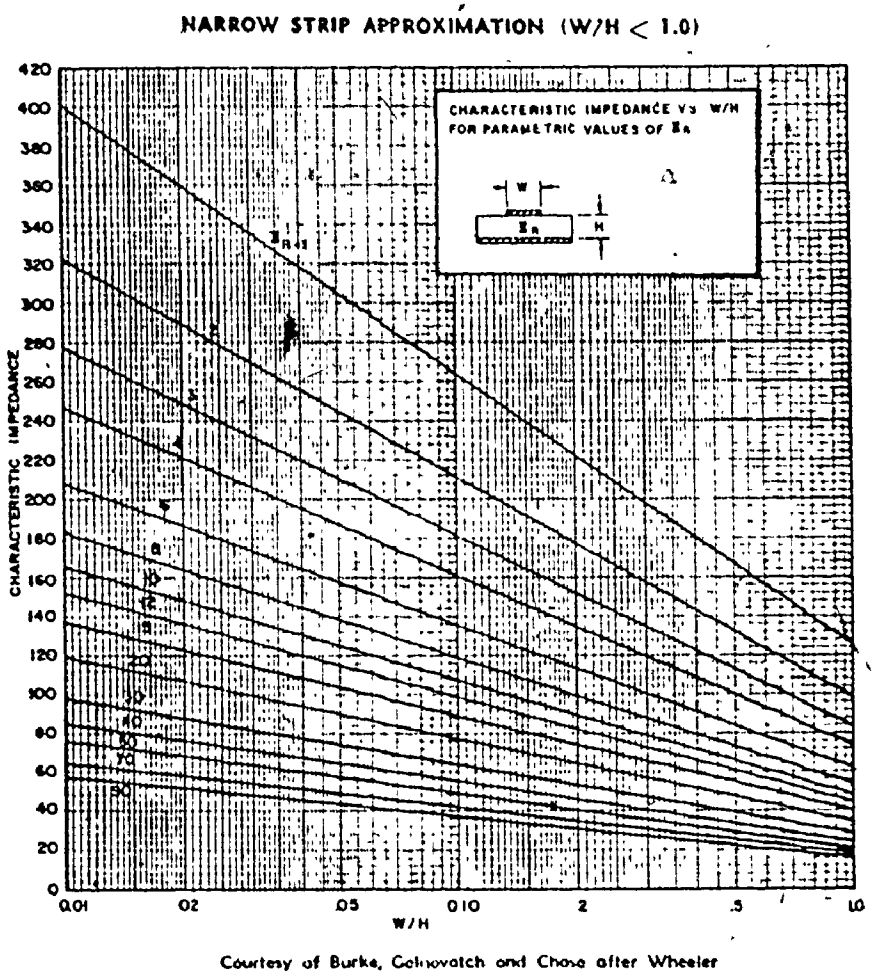

Figure A.1 Microstrip Characteristic Impedance Curves [30]

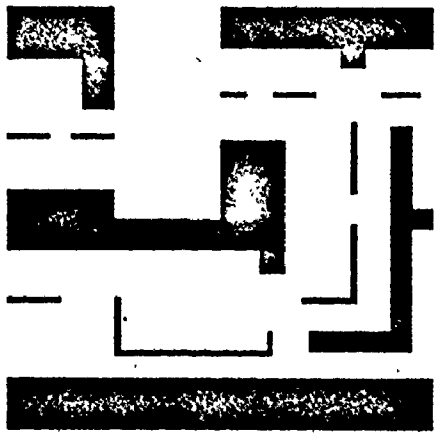

Figure A.2 Mask of Oscillator Circuit Board on Red Rubylith

(3) The board was then dried and baked in an oven at 85°C to ensure that the surface was perfectly dry.

(4) One side of the board was then evenly coated with a thin (≃ 5000 Å) layer of AZ-1350-B (Azoplate) positive photoresist by means of a spinner.

(5) The board was baked for 15 minutes at 85°C to dry the resist layer.

(6) The dried board was then positioned resist-side up approximately 12" under an ultraviolet light source. (650 watt projection lamp). The rubylith mask was then positioned over the board and the pattern was exposed for 5 minutes.

(7) The exposed resist was developed with AZ-1350-B developer for 90 seconds and then rinsed with deionized water for 2 minutes.

(8) The board was then baked again for 15 minutes at 85°C to ensure that the resist layer could withstand the etchant.

(9) Paraffin was used to adhere the board to a small piece of plexiglass which ensured that the ground plane was protected from the etchant and also that the board would not warp.

(10) The board was etched in a moderately warm, saturated solution of ferric chloride for approximately 20 minutes. After etching, the board was rinsed with acetone followed by a 2 minute rinse in deionized water.

APPENDIX II

DETERMINATION OF LOAD IMPEDANCE USING SINGLE-STUB MATCHING

Consider the transmisison line set-up shown in Figure A.3. A variable short-circuit tuning stub is inserted at point B along the transmission line, and following B a variable coaxial line is terminated at C with the SAW transducer under test. All of the transmission line components consist of air lines and hence the phase velocity is approximately the speed of light. Let the SAW transducer present a normalized load admittance of $Y_L = a + jb$ mhos at the point C. The purpose of single-stub tuning is to adjust the lengths L_1 and L_2 such that the load appears to be matched to the characteristic impedance of the system at the point B. The length L_2 is adjusted until the normalized admittance at point B is of the form:

$$Y_B = 1 + jx \qquad (b.1)$$

The remaining task is to adjust the stub length L_1 such that the reactance presented at point B by the stub is $Y_{B(stub)} = -jx$. The total admittance at point B will then become:

$$Y_B' = Y_B + Y_{B(stub)} \qquad (b.2)$$

$$= 1 + jx - jx$$

$$= 1$$

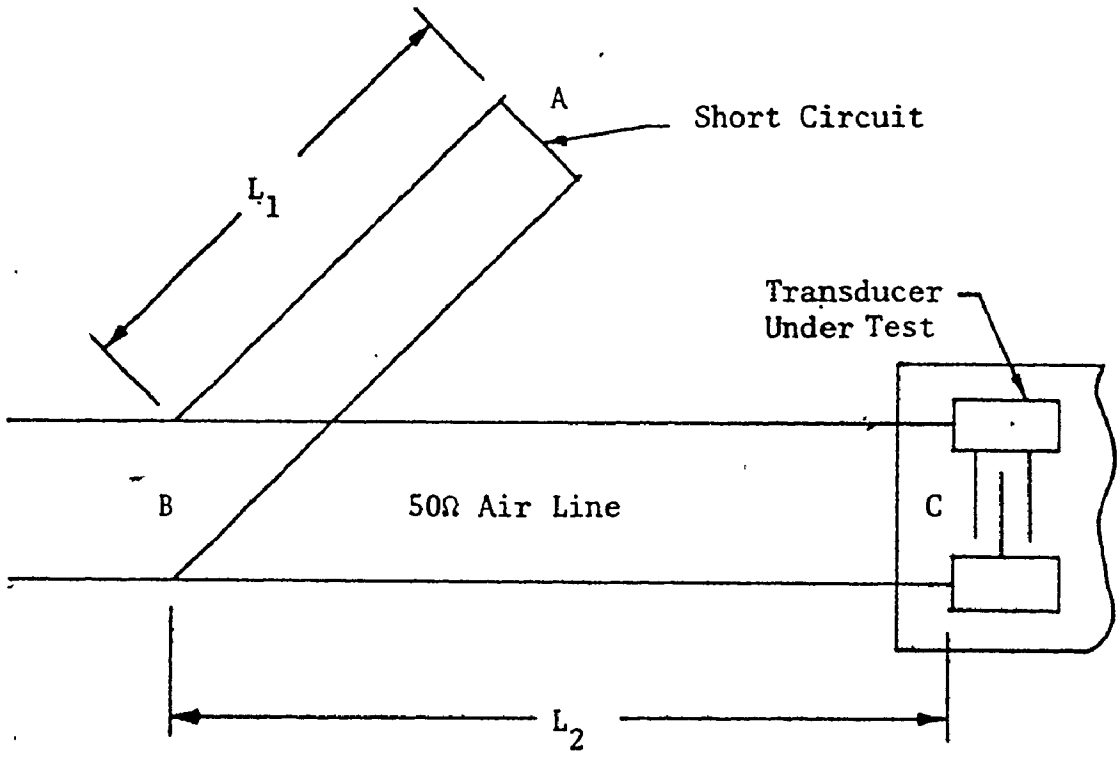

Figure A.3 Single-Stub Matching Technique to Determine Load Impedance

A matched condition is thus effected. When the load admittance is unknown, the entire process can be applied in reverse, given the tuning lengths L_1 and L_2. Tuning lengths and admittance values are usually derived from a Smith chart, however the following analysis was used in a computer program which calculated the load impedance, given the centre frequency, L_1 and L_2.

Starting at the point A in Figure A.3, the reflection coefficient for the short circuit is $\rho_A = 1\underline{/180°}$. If L_1 is given in cm, then the equivalent length L_1' in degrees is:

$$L_1' = \frac{9 f_o L_1}{375} \qquad (b.3)$$

where f_o = the centre frequency of operation

Therefore the resulting reflection coefficient at point B due to the stub is:

$$\rho_B = 1\underline{/180 - L_1'}$$

The equivalent reactance at this point due to the stub is then given by:

$$Y_{B(stub)} = \frac{1 - \rho_B}{1 + \rho_B} \qquad (b.4)$$

$$= j\gamma$$

Since a matched condition exists, the normalized admittance at the point B must be of the form: $1 + jx$, which implies that $x = -\gamma$, hence

$$Y_B = 1 - j\gamma \tag{b.5}$$

The length L_2 is now similarily converted into degrees by the relation:

$$L_2' = \frac{9f\ L_2}{375} \tag{b.6}$$

Equation (b.5) must then be expressed in terms of reflection coefficient by the following relation:

$$\rho_B' = \frac{1 - Y_B}{1 + Y_B} = \xi/\phi \tag{b.7}$$

Therefore the resulting reflection coefficient at the load (point C) is:

$$\rho_c = \underline{\xi/\phi + L_2'} \tag{b.8}$$

The normalized load impedance is then given by:

$$Z_N = \frac{1 + \rho_c}{1 - \rho_c} \tag{b.9}$$

Denormalizing, this yields a transducer impedance of the form:

$$Z_L = \alpha + \frac{1}{j\beta} \tag{b.10}$$

The form of equation (b.10) implies the series circuit representation of a SAW transducer, and the radiation resistance and total capacitance can be obtained directly from the following:

$$R_a = \alpha$$

$$C_T = \frac{\beta}{2\pi f_o}$$

REFERENCES

1. B.A. AULD, "Acoustic Fields and Waves in Solids", Volume 1, Wiley-Interscience Publication, 1973.
2. M.G. HOLLAND, L.T. CLAIBORNE, "Practical Surface Acoustic Wave Devices", Proceedings of the IEEE, Volume 62, No. 5, May 1974, pp. 582-602.
3. M.H. EL-DIWANY, "Surface Acoustic Wave Bandpass Filter Synthesis and Design", M. Eng. Thesis, McMaster University, May 1975.
4. G.W. FARNELL, E.L. ADLER, "An Overview of Acoustic Surface-Wave Technology", Report to Communications Research Centre, DSS Contract 36001-3-4406, McGill University.
5. D.B. WOHLBERG, G.W. FARNELL, "Proceedings of the Canadian Workshop on Acoustic Surface Waves", Communications Research Centre, Report No. 1260, June 1974.
6. M.F. LEWIS, "Surface Acoustic Wave Oscillators", Microwave Systems News, p. 29, Dec./Jan. 1974.
7. P.M. GRANT, J.D. ADAM, J.H. COLLINS, "Surface Wave Device Applications in Microwave Communication Systems", IEEE Transactions on Communications, Volume COM-22, No. 9, Sept. 1974.
8. M.F. LEWIS, "The Design, Performance and Limitations of SAW Oscillators", International Specialist Seminar on Component Performance and Systems Applications of Surface Acoustic Wave Devices, IEE Conference publication No. 109, p. 63.

9. S.J. KERBEL, "Design of Harmonic SAW Oscillators without External Filtering and New Data on the Temperature Coefficient of Quartz.", Ultrasonics Symposium Proceedings, Nov. 1974, Pub. no. 74 CHO 896-1SU.

10. H. ENGAN, "Excitation of Elastic Surface Waves by Spatial Harmonics of Interdigital Transducers", IEEE Transactions on Electron Devices, Volume ED-16, No. 12, Dec. 1969.

11. E.J. STAPLES, J.S. SCHOENWALD, R.C. ROSENFELD, C.S. HARTMANN, "UHF Surface Acoustic Wave Resonators", 1974 IEEE Ultrasonics Symposium Proceedings, pp. 245-252, 74 CHO 896-1SU.

12. R.C. LI, R.C. WILLIAMSON, D.C. FLANDERS, J.A. ALUSOW, "On the Performance and Limitations of the Surface-Wave Resonator using Grooved Reflectors." 1974 IEEE Ultrasonics Symposium Proceedings, pp. 257-262, 74 CHO 896-1SU.

13. W.L. SMITH, "Some General Properties of Resonator Stabilized Feedback Oscillators", 1974 IEEE Ultrasonics Symposium Proceedings, pp. 773-777, 74 CHO 896-1SU.

14. T.W. BRISTOL, "Analysis and Design of Surface Acoustic Wave Transducers", IEE International Specialist Seminar on Component Performance and Systems Applications of Surface Acoustic Wave Devices, pp. 115-130, Scotland, Sept. 1973.

15. J. CRABB, M.F. LEWIS, J.D. MAINES, "Surface Acoustic Wave Oscillators: Mode Selection and Frequency Modulation", Electronics Letters (GB), pp. 195-197. (17 May, 1973)

16. J. ZUCKER, "Surface Acoustic Wave Devices", Profile, G.T.E. Laboratories Inc., No. TWO/1974.

17. R. JONES, J. SCHELLENBERG, W.J. TANSKI, R.A. MOORE, "Transplexing SAW Filters for ECM, Part 1", Microwaves , p. 43, Dec. 1974.

18. R.C. WILLIAMSON, "Problems Encountered in High-Frequency Surface-Wave Devices", IEEE Ultrasonics Symposium Proceedings, pp. 321-328, Nov. 1974, 74 CHO 896-1SU.

19. A.J. SLOBODNIK, JR., T.L. SZABO, "Design of Optimum SAW Delay Lines", IEEE Transactions on Microwave Theory and Techniques, pp. 458-462, April, 1974.

20. H.I. SMITH, "Fabrication Techniques for Surface Acoustic Wave and Thin-Film Optical Devices", Proceedings of the IEEE, Volume 62, No. 10, pp. 1361-1387, Oct. 1974.

21. A.J. SLOBODNIK, JR., "UHF and Microwave Frequency Acoustic Surface Wave Delay Lines: Design", Air Force Cambridge Research Laboratories, AFCRL-TR-73-0538, Aug. 1973.

22. M.B. SCHULZ, M.G. HOLLAND, "Surface Acoustic Wave Delay Lines with Small Temperature Coefficient", Proceedings of the IEEE, pp. 1361-1362, Sept. 1970.

23. S.P. KWOK, "UHF Broadband Amplifier Design", Motorola Semiconductor Products Inc. Application Note AN-406.

24. H.L. KRAUSS, C.W. ALLEN, "Designing Toroidal Transformers to Optimize Wideband Performance." Electronics, pp. 113-116, August 16, 1973.

25. M.B. SCHULZ, M.G. HOLLAND, "Materials for Surface Acoustic Wave Components", IEE Seminar on Component Performance and Systems Applications of Surface Acoustic Wave Devices, pp 1-10, Sept. 1973.

26. J.F. DIAS, H.E. KARRER, J.A. KUSTERS, J.H. MATSINGER, M.B. SCHULZ, "The Temperature Coefficient of Delay-Time for X-Propagating Acoustic Surface-Waves on Rotated Y-Cuts of Alpha Quartz", IEEE Transactions on Sonics and Ultrasonics, Volume SU-22, Number 1, Jan. 1975.

27. E.C. JORDAN, K.G. BALMAIN, "Electromagnetic Waves and Radiating Systems", Prentice-Hall Inc. Publisher, Second Edition, 1968, pp. 306-309.

28. R.E. COLLIN, "Foundations for Microwave Engineering", McGraw-Hill Book Company, Copyright 1966, pp. 208-211.

29. R. BALE, M.F. LEWIS, "Improvements to the SAW Oscillator", IEEE 1974 Ultrasonic Symposium Proceedings, 74 CHO 896-1SU, pp. 272-275.

30. T.S. SAAD, "Microwave Engineers Handbook, Volume 1", Artech House, Inc., Copyright 1971.